This paper is clear and well presented with a valid methodology to simulate FIR radiances from the Mid-IR. However it is not clear what is the need for this as radiative transfer models can make the same simulation with probably better accuracy.

One point that needs to be made here is that radiative transfer tools have not been extensively validated in the far infra-red. The evaluation which has been done is limited by the available measurements covering this spectral region, which are not extensive – indeed the REFIR-PAD dataset is the only such dataset covering the full FIR spectral range over an extensive (multi-season) period of time.

A related question then becomes why one would attempt to extend the MIR to cover the FIR using the approach discussed here rather than simply using the data to directly evaluate the LBLRTM code over this range. We argue that several authors have described similar techniques, then actively implemented them to extend satellite mid-infrared radiances to cover the FIR (Turner et al., 2015, Huang et al., 2013, Huang et al., 2008). While we are considering a different viewing geometry, and thus might expect a different pattern of spectral correlations or patterns to emerge, in this case we are able to actually test the level of spectral agreement obtained with real observations, something not possible in the earlier studies due to the lack of space-based FIR spectral measurements. Indeed, while both earlier studies show good agreement with observations at the broadband level, comparisons between an extended AIRS dataset and GCM simulations show that such agreement could still hide compensating effects across the spectrum.

Huang, X.; Yang, W.; Loeb, N. G. & Ramaswamy, V., Spectrally resolved fluxes derived from collocated AIRS and CERES measurements and their application in model evaluation: Clear sky over the tropical oceans, Journal of Geophysical Research: Atmospheres, 2008, 113, n/a-n/a

Huang, X.; Cole, J. N. S.; He, F.; Potter, G. L.; Oreopoulos, L.; Lee, D.; Suarez, M. & Loeb, N. G., Longwave Band-By-Band Cloud Radiative Effect and Its Application in GCM Evaluation, Journal of Climate, 2013, 26, 450-467

Turner, E. C.; Lee, H.-T. & Tett, S. F. B., Using IASI to simulate the total spectrum of outgoing long-wave radiances, Atmospheric Chemistry and Physics, 2015, 15, 6561-6575

The other major limitation is the results are only valid for radiances over Antarctica which limits the interest as to be of real value to climate modellers a more global application of this technique is required. Hence before accepting publication of this paper I would like to see a much clearer explanation for why this technique would be useful given its limitations outlined in the paper.

The main reason why the study has only been performed over Antarctica is that, as noted above, the only instrument which has measured the complete FIR downwelling spectral radiance over an extended period of time is the REFIR-PAD located at Antarctica. We anticipate that, given the very specific meteorological conditions seen at this location the relationships we find here may well not hold for other locations but our goal is to use the existing data as a starting point to see whether the approach is actually viable, and what the key drivers of uncertainty are. This is timely because there is at least one mission (FORUM) that could provide the global observational data needed to derive such a relationship (for top of atmosphere radiances) in future. This could then be retrospectively applied with more confidence to numerous older, spectral MIR only, satellite observations.

It is also worth noting that Turner et al. (2015) use only one regression relationship regardless of atmospheric state (i.e. they assume the relationship derived from a limited number of radiative transfer simulations is robust across all conditions) while Huang et al. (2008) derive clear-sky FIR estimates from MIR observations based on principal component analysis of a more extensive data set of simulated spectra, but for relatively coarse intervals of surface temperature, precipitable water and lapse rate.

Also a demonstration of the technique over a wider range of atmospheric conditions is needed.

If the reviewer means a wider range of clear-sky conditions then obviously we are limited by the typical range of conditions seen at Concordia, which have effectively been sampled by considering a whole year of data. If the comment is more towards the fact that only clear-sky conditions are considered this is mainly because, as noted above, our goal is to determine whether the technique is viable, not to develop a method that can be applied to all-conditions and locations. In principle, if we see large differences at this point, for relatively constrained conditions, it is unlikely that a single set of regression coefficients will yield acceptable results in all locations, even if derived from simulations sampling all conditions. A second factor is the difficulty in discriminating between different types of cloud/precipitation (e.g. cirrus, diamond dust, etc.) and constraining the cloud microphysics – which we would expect to have a strong influence on the observed spectral shape across the infrared. Since the approach relies on forward modelling, without this information we would have the concern that our forward simulations were not really representative of the observed conditions and hence the statistical relationships derived between the MIR and FIR could not be expected to capture the true behaviour.

Overall impression

The authors note, correctly, the sparsity of far-infrared hyperspectral radiance measurements compared to the mid-infrared. Given the important role of the far-infrared in climate and energy budget studies it is a worthwhile endeavour to seek to improve our knowledge of the full infrared spectrum. The methodology of Turner et al. (2015), which entails using mid-infrared predictor channels to infer far-infrared spectral radiances, is applied to a dataset of Antarctic downwelling longwave radiances (REFIR-PAD). The paper tests whether the methodology can successfully extend/extrapolate mid-infrared spectra into the far-infrared.

Within certain conditions the authors show reasonable skill in predicting the FIR spectrum from MIR data. Notwithstanding some points about how this works in practice (see below) I think the general idea has applicability in climate science where FIR data are lacking. The authors note that there is renewed interest in the remote sensing community in spectrally resolved FIR measurements (specifically the candidate ESA mission FORUM). I hope the authors can address the more detailed points raised below.

Substantive points

1. Page 3, line 27. "In the study, only clear-sky cases from 2013 are used." There may be good reasons for this choice, but these are not clear. Please explain why this data selection was made.

The purpose of this study is to investigate the statistical correlations between the mid-infrared and far-infrared portion of the downwelling spectra in Antarctica. This can be done by exploiting a dataset covering the seasonal variability during a whole year. The 2013 dataset was chosen since it represents one of the years with a very large number of spectra, with a good estimate of the spectral error.

Our reason for focusing on clear-sky conditions only is as noted in the responses to reviewer 1: our goal is to determine whether a regression type extension technique can give reasonable accuracy when compared to real observations, not to develop a method that can be applied to all-conditions and locations. In principle, if we see large differences at this point, for relatively constrained conditions, it is unlikely that a single set of regression coefficients will yield acceptable results in all locations, even if derived from simulations sampling all conditions. The main variables which contribute in both the FIR and MIR portions of the terrestrial spectrum are water vapour and clouds. For this study we want to separate these two contributions, since the cloud effect needs to be investigated separately and more accurately: in particular a lack of ancillary observations means it is difficult to discriminate between different types of cloud/precipitation (e.g. cirrus, diamond dust, etc.) and constrain the cloud microphysics – which we would expect to have a strong influence on the observed spectral shape across the infrared. Since the approach relies on forward modelling, without this information we would have the concern that our forward simulations were not really representative of the observed conditions and hence the statistical relationships derived between the MIR and FIR could not be expected to capture the true behaviour.

2. Methodology, page 5. There are various differences between the published method (T15) and the way it is applied here. In T15 IASI data (upwelling radiances) are used cf. downwelling REFIR-PAD data; T15 data are restricted (it seems, on quick read) to between 30S and 60N cf. cold/dry Antarctic conditions here; T15 find maximum correlations either side of peak water vapour absorption at 1600 cm-1 while REFIRPAD is restricted to below 1400 cm-1. These are not commented upon.

Text has been added in the introduction to highlight the differences between T15 and our study. We start with the fact that T15 uses LBLRTM simulations to create the prediction model but without the possibility to verify that the prediction model is consistent with observational spectra since there are no FIR observations from space. Therefore, the comparison of the extended spectra is also impossible to realise in T15 and only broadband validation is performed. T15 wavenumbers of maximum correlation are also recalled in section 3.2.

In particular I would like the authors to comment on the general applicability of their scheme for global climate studies when this paper deals exclusively with polar conditions.

Please see our first response above and also those to reviewer 1, which highlight how our intention was not to create a generally applicable scheme but rather to test whether such a technique could generate realistic spectral radiances when compared to real observations. As such we would not necessarily expect the spectral relationships we see to hold under conditions that are substantially different to those sampled here: for example, the additional water vapour seen at lower latitudes would be expected to have a substantially greater impact in the FIR micro-windows than the main atmospheric window. We have now made this intent clearer in the revised manuscript.

3. The method relies on finding a single predictor MIR wavenumber for each FIR wavenumber. This is straightforward and as published in T15. However, there may be potential downsides to using single frequencies, particularly when the same predictor is selected multiple times and in cases of instrument noise. Have the authors considered whether a weighted average or linear combination of the most highly correlated channels might work better as a predictor?

Indeed, updating the method using a weighted average or linear combination of the most highly correlated channels could improve the results, especially at wavenumbers lower that 170 cm^{-1} where the correlation decreases (figure 2(b) and 5(d)). We would not expect much changes between 200 and 450 cm^{-1} since the correlation is higher. However, we think our approach works well enough that adding more complexity at this stage is not necessary.

4. Some plots (Figs 4, 6) show standard errors to represent the uncertainty. I am uncomfortable with this, as it implies the expected error in the method can be reduced to the mean error with an

arbitrarily large sample. The uncertainty is better represented as the example in Fig. 4 (a) where the difference between spectrum and extension in microwindows near 240/260/270 cm-1 is about 10 r.u. Elsewhere (Table 1) you quote one standard deviation which seems more appropriate to me.

Actually, the standard error as used in figure 4 and 6 stands for the standard deviation of the extension among the set of spectra considered. Therefore, the figures are consistent with table 1. It was set as standard error in order to avoid confusion between the standard deviation of a single REFIR-PAD spectrum and the standard deviation relative to the extension of a specific set. However, it has been corrected in the updated version of the article.

5. Page 8, Eq. (3). You add noise according to the REFIR-PAD standard deviation, but you discount correlated errors e.g. the calibration error in Fig. 1. If you want to represent the instrument uncertainty shouldn't this be included?

We used the standard deviation, and this does actually include the NESR in its computation. Rizzi et al. (2016) uses the maximum between CAL + NESR and σ. Our results have been updated to be consistent with MAX(SQRT(CAL^2+$NESR^2$), σ), as expressed with equation 3.

6. You show (Fig. 5) very different choices of predictor channels when using noiseless and noise-added LBLRTM spectra (the latter look very like those found from REFIRPAD in Fig. 2). You say in the discussion and conclusions that including the effects of noise is important to improve the prediction model. But I think this avoids the interesting question of why the noise-free LBL extension fails (but why LBN and LBC seem to work). Plausibly it comes down to the choice of predictor channels which are heavily skewed towards 1400 cm-1 in the LBL case. Just because channels are correlated doesn't mean they have a linear relationship. It might be interesting to see an equivalent of Fig. 3 for an LBL case.

We believe that the fact that LBL fails to extend correctly to the FIR originates from the lack of correlation in REFIR-PAD data at the wavenumbers that maximise the correlation for LBL. When comparing the correlation see in figure 5(c) and the corresponding blue/yellow area in figure 2(a), the correlations in REFIR-PAD data do not exceed 0.5.

The equivalent of figure 3 for LBL cases is shown below (figure r1), exhibiting, as expected, a much higher correlation coefficient. The predictor wavenumber here is 1376.00 cm^{-1}. Most of the highly correlated LBL wavenumber duos follow this shape, close to a linear relationship.

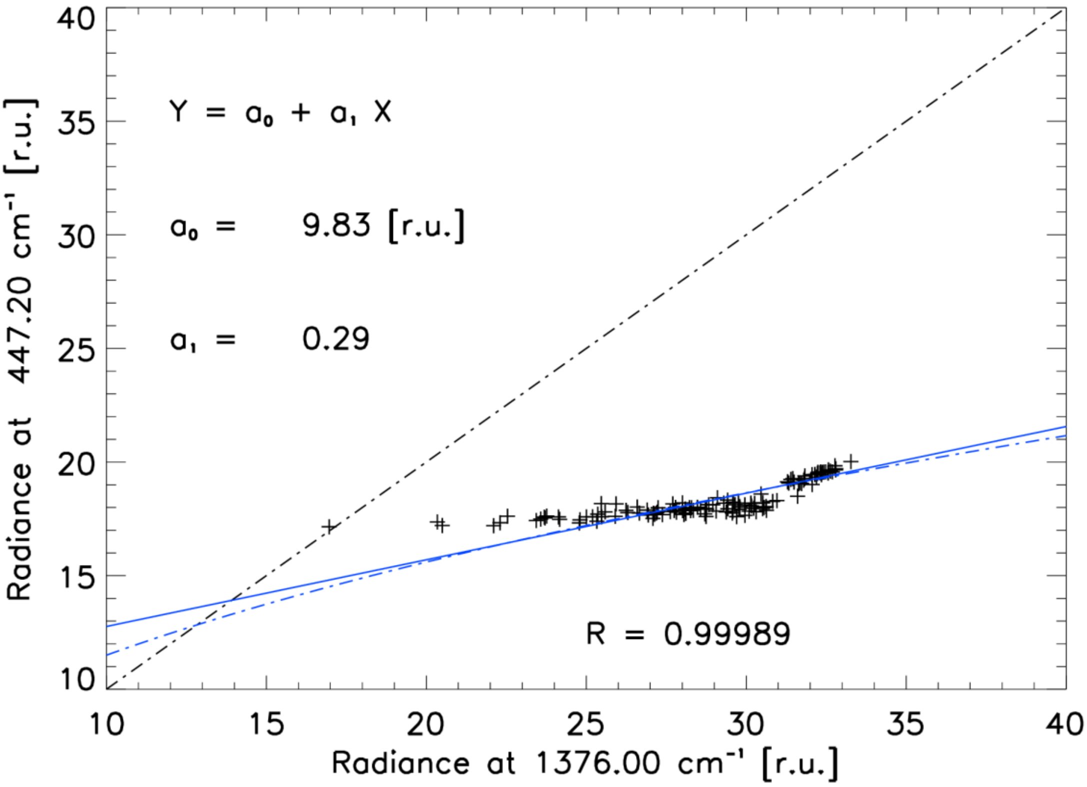

Figure r1: FIR radiances at 447.20 cm-1 against predictor MIR radiance at 1376.00 cm-1 for simulated LBLRTM cases (same as figure 3).

7. If instrument (random) noise is critical in your method there may be benefit in noise filtering the measured spectra. Methods exist for doing this, e.g. via principal component analysis. I anticipate this may be beyond the scope of the present study but may be worth pursuing in future work.

Thank you for the suggestion. Indeed, this could be used in future work along with the optimisation of the predictor wavenumbers.

Minor points

1. **Page 2, line 9. Typo “vvvhave”.** ☑
2. **Page 3, line 22. “One calibrated spectra”, strictly “spectrum”.** ☑
3. **Fig. 3, I assume the dot-dashed line is a 1:1 line but this is not stated.** ☑
4. **Page 10, line 8, you refer to “figure 5 (b)” when it looks like (c)?** ☑

Overall comments

The paper “Can downwelling far-infrared radiances over Antarctica be estimated from mid-infrared information?” demonstrates a method for estimating downwelling far-IR spectral radiances at the surface in Antarctica from mid-IR radiances (both measured and calculated) at that location. Although the main result in the paper is adequately presented, overall the paper suffers from significant motivational and methodological issues.

This study is presented as similar to the TOA-based study of Turner et al. (2015). The need for the results presented in the earlier study can be straightforwardly seen. There exist many millions are mid-IR spectral radiance measurements from satellites (IASI, CrIS, AIRS, TES) without far-IR counterparts, and the construction of far-IR simulated radiances consistent with the mid-IR observed radiances could be very useful. That these observations are global and span more than a decade also attest to their utility. However, the same is not the case for surface radiances. This paper does not really attempt to make an argument that the development of this technique is likely to be relevant or the lessons learned from this study will be able to be applied to something relevant. There is no global set of mid-IR ground-based spectral radiometers for which this technique would be useful. The closest is the many AERIs that have been deployed, but the vast majority are located in regions with high enough water vapor so the far-IR is opaque and a simple surface air temperature measurement will suffice to predict the far-IR radiances. Only the few AERI datasets from high-latitude or –altitude might be spectrally extended using a variant of this technique, but even that application begs the question as to what would be the need to adequately fill in the far-IR record for these deployments. A weak motivational argument is made by alluding to the FORUM mission, but this is a satellite-based instrument. Without some adequate motivation, there is no real reason for this paper to be published.

As mentioned in the introduction, T15 applied the methodology to nadir radiance measurements from the IASI instrument and evaluated their approach by comparing spectrally integrated radiances across the infrared with measurements from the CERES broadband radiometers. Overall mean broadband agreement has been shown to be encouraging but the evaluation technique precludes the identification of any compensating biases within the FIR itself. Our intention here was to test whether it is possible to use such a technique to infer spectral FIR radiances from MIR radiances, using observational spectra to validate the results obtained. Given the comments of this, and the other reviewers, we did not make it clear enough in the original manuscript that the goal was not to develop a new technique to be applied to all ground-based observations (of which we are well aware there are few) but to test the general principle of the approach.

The methodology employed is also problematic. In a dry location like Antarctica, far-IR radiances are primarily determined by the temperatures and water vapor amounts in the lowest layers of the atmospheres. Therefore, a technique to predict far-IR radiances using a single observed mid-IR radiance would ideally use a frequency that also is sensitive to these atmospheric conditions. However, the paper indicates that any such REFIR-PAD channels (1300-1400 cm-1) are too impacted by noise to be very useful for this application. Therefore the method that is arrived at predominantly uses frequencies in the CO2 band, measurements that basically are sensitive just to the temperatures at the levels very close to the instrument. (The text incorrectly suggests that water vapor is also important in this spectral region.) Therefore, this result in the paper can be oiled down to most important consideration in simulating far-IR radiances, given the noise in REFIR-PAD mid-IR water vapor channels, is getting the near-instrument temperature correct.

The reviewer is absolutely correct that in an ideal world one would want to exploit observations from 1300-1400 cm^{-1} (or even higher wavenumbers to properly sample the water vapour rotation-vibration band) and that we are limited by the REFIR-PAD noise here. However, while we agree that for the noisy case most of the 'skill' in the extension to wavenumbers below 450 cm^{-1} is mainly coming from near surface temperature (via CO_2 emission at around 700-720 cm^{-1}), between 450-600 cm^{-1} there is certainly information from water vapour variability and profile (see figures r2 and r3 below which shows the impact of variations in profile for a typical radiosonde profile from Antarctica across the full spectral range of REFIR-PAD). We also note that at no point in the original manuscript did we state that water vapour was important in the CO_2 band wings – in fact we explicitly called them just that – however there are small water vapour features within this range (see zoomed in plot r4 and r5) and some of the predictor wavenumbers will include their contribution.

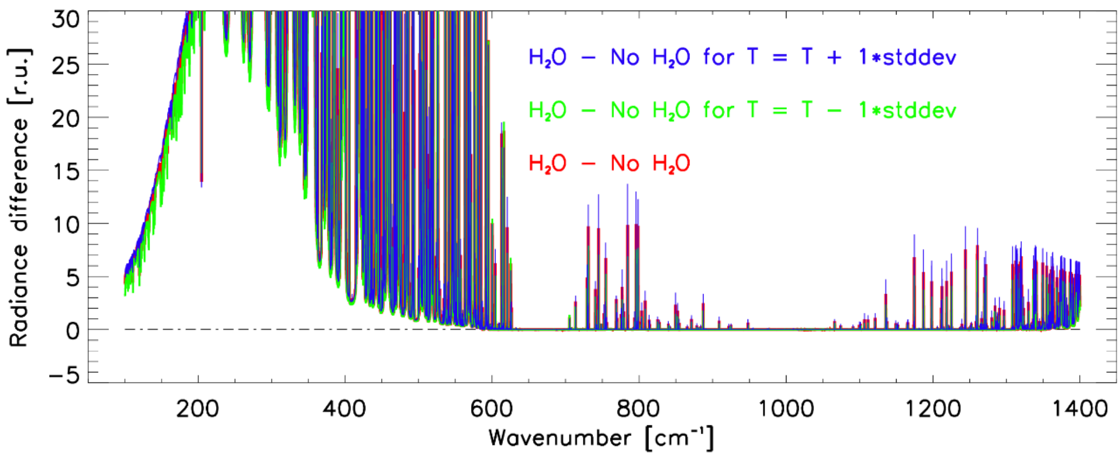

Figure r2: Differences between downwelling radiances computed using an atmospheric profile with and without water vapour (in red), and for 2 cases of temperature perturbations (+/- 1 standard deviation, respectively in blue and green, computed over the whole set of atmospheric profiles used in this study).

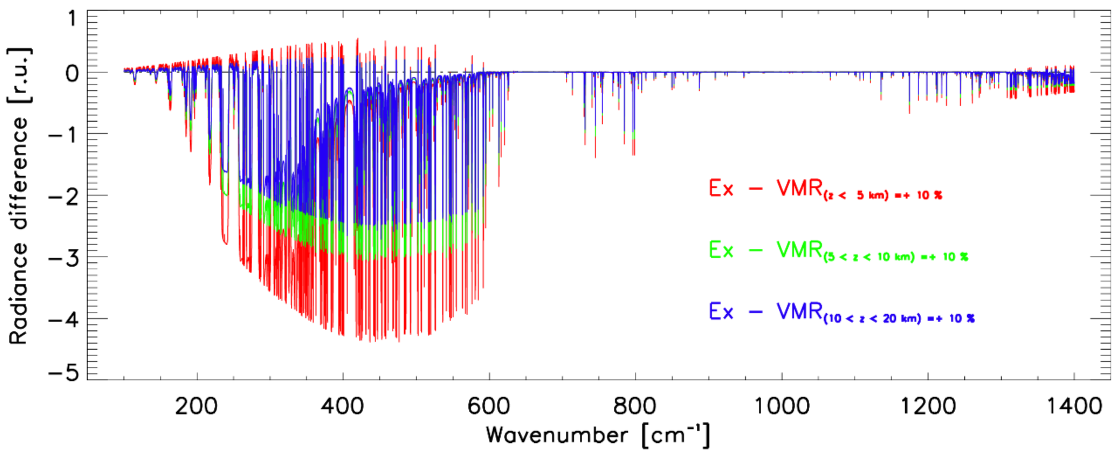

Figure r3: Differences between downwelling radiances with local perturbations in the water vapour profile. In red, the VMR below 5 km has been increased of 10 %, in green (blue), the VMR between 5 and 10 km (between 10 and 20 km) has been increased of 10 %.

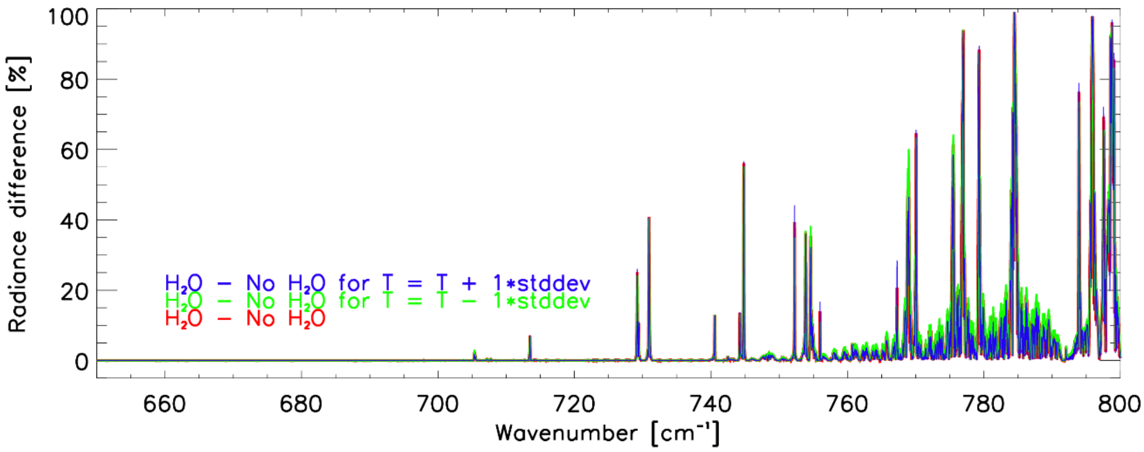

Figure r4: Relative difference for the same cases as figure r2, between 650 and 800 cm-1.

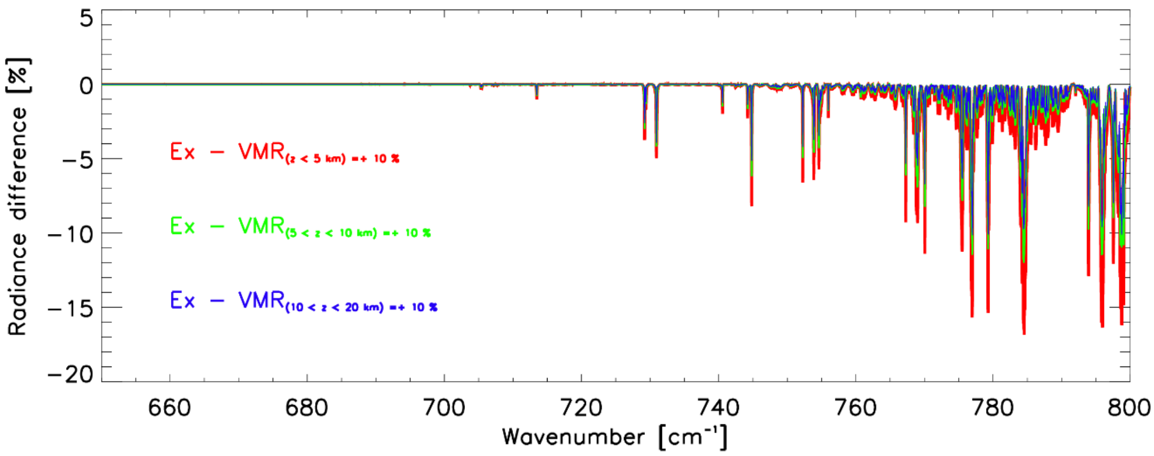

Figure r5: Relative difference for the same cases as figure r3, between 650 and 800 cm-1.

Understanding the result in this context should give the authors some pause in any assessing the importance of this result – if the simulated far-IR radiances are independent of the water vapor profile, how useful and information-laden can they be? Given the ease these days of doing non-simple optimization, it's unclear why the authors did not determine an optimal linear combination of the radiances at multiple channels for each far-IR radiance. By definition, this would obtain better results than using a single channel and allow the use of spectral points sensitive to both temperature and water vapor.

As noted above (and shown by the figures) there is clearly sensitivity to the water vapour profile in the far-infrared and also, increasingly from wavenumbers from around 710 cm^{-1} and above, even for this ground-based viewing geometry.

We do appreciate that including multiple channels in the predictor approach may well have been beneficial (noise permitting) and this is now explicitly stated in the revised manuscript and would be an avenue to pursue in future when developing a more generic approach.

The comments above mainly apply to the results in the paper about using observed mid-IR radiances to simulate far-IR radiances. The paper also has results for using calculated mid-IR radiances to

obtain far-IR radiances. It's not clear if these results would be useful since if one were already doing calculations and wanted far-IR radiances, why not compute them directly?

Essentially this is the same point as one raised by reviewer 1. If one had complete confidence in the ability of radiative transfer codes to correctly simulate far-infrared radiances then of course one could use them across the whole infrared range. In practice we simply do not have this confidence (as evidenced by the numerous updates to water vapour spectroscopy in this region over time as new observations become available) due to the very limited number of measurements. Moreover, even if we had complete confidence, as the reviewer themselves state '**There exist many millions are mid-IR spectral radiance measurements from satellites (IASI, CrIS, AIRS, TES) without far-IR counterparts, and the construction of far-IR simulated radiances consistent with the mid-IR observed radiances could be very useful'.** It would be a Herculean task to simulate every individual spectrum, and in many cases sufficient knowledge of the underlying conditions would not be available to do so, so deriving a robust statistical approach to perform the task is attractive. Ultimately one would want to both (a) validate our understanding of the far-IR and (b) test any such statistical approach with suitable observations, such as those proposed via the FORUM mission.

Our point in showing the noise-free LBLRTM results (applied to the observations) is to indicate how instrument noise affects both the choice of predictor wavenumbers from a noise-free case, at least in 'model' world.

Specific comments by page, line. More important comments denoted by *:
Section 1
2, 3 – perhaps use "as much of as N %" instead of "significant" since "significant" is pretty subjective (and the fraction is probably less than 50%)

Changed for "allow as much as 45 % of FIR radiation emitted from the ground to escape directly to space" (from Harries et al., 2008).

2,9 – some extra "v" characters are present ☑

2, 13 – It might be worth mentioning the RHUBC campaign (papers by Turner, Mlawer) ☑

3,1-3 – A potential satellite mission is not relevant to this paper's purpose since this analysis only applies to ground-based measurements. It may be relevant to the T15 paper, but not to this paper.

See answer to point 14, 24-29.

Section 2
3,15 – The REFIR_PAD goes up to only 1400 cm-1, so it's hard to see how that could be a "complete longwave dataset."

"Complete" has been removed.

4,9 – Perhaps start this sentence "Each radiosonde records data every 2 seconds: : :". The current wording might be taken as sondes are launched every 2 seconds.

We could not find the sentence "each radiosonde records […]" but the closest sentence has been rewritten for "During a radiosonde launch, data are recorded every 2 seconds, corresponding to around 800 measurements […]"

4,19 – Perhaps get rid of "developed by" and change Clough et al. into a regular reference (i.e. in parentheses). The current wording makes it seem like the model was developed around 2006. ☑

5,1 – In the far-IR, the linefile has substantial modifications to the HITRAN 2016 widths following Delamere et al. and Mlawer et al. The latter study also led to MT_CKD_3.0. The text says "includes modifications", but doesn't specify what the modifications were in reference to (i.e. modifications to what?). Since the RHUBC-II results are primarily based on REFIR-PAD measurements, it is probably worth mentioning when introducing the model.

Following http://rtweb.aer.com/lblrtm_whats_new.html , I rewrote as: "[…] code MT_CKD_3.0 which includes up-to-date H2O foreign continuum from 0-600 cm-1 and the self continuum in the microwave that resulted from an analysis of measurements taken at the ARM RHUBC-II campaign and a re-analysis of RHUBC-I measurements."

5,22 – Do the conditions have to be clear for the entire period between when the sonde is launched through the REFIR-PAD measurement time?

From Rizzi et al., 2016, the approach to separate clear sky to cloudy sky uses radiances ratio as specific wavenumbers. Therefore, it implies that the cloud condition does not change much during the measurement time. Daily lidar quick looks have also been manually used to verify the classification. In addition, since the acquisition time is 6.5 min, it seems safe to assume that the weather conditions are stable.

5,25 – random subsampling?

Yes, the subsampling was performed with running random indexes. A few sets of random indexes has been tested to check if the subsampling had an impact and it did not.

Section 3
6,8 and Fig. 1 – Specify whether these results are for linear or log.

The correlation map is built by looking at the correlation between a vector based on the radiances at a specific FIR wavenumber and the corresponding vector based on the radiances at a specific MIR wavenumber. Therefore, there is no linear or log consideration at this stage.

Same for figure 1 where the example originates from the data and not an extension. The linear and log consideration applies for figures 3, 4 and 6. In these cases, the text specifies linear or log. But this has also been added to the figure captions.

***9,2 – The noise added is between -1 and 1 times the standard deviation of the measured noise at each frequency. Doesn't this underestimate the actual noise? Why not use the chosen random number to sample from a normal distribution with that standard deviation?**

I am not sure that I understood properly your suggestion since a normal distribution with a standard deviation of σ is the same of a normal distribution with a standard deviation of 1 times the standard deviation σ (our case):
np.random.normal(mu, sigma, 10000) ≡ np.random.normal(mu,1.0, 10000)*sigma

Also, does the actual noise have spectral correlation? (i.e. if a case is higher than the mean in the MIR, is it likely to be higher than the mean in the FIR?). If so, then not taking that into account in the method may lead to inferior results for the LBLRTM+noise compared to using a pure measurement approach.

The error of REFIR-PAD measurements were considered completely uncorrelated. This is very common in most of previous analysis of this kind of measures from other instruments similar to REFIR-PAD, see for example (Turner, 2005). In this study we considered the standard deviations of the mean of 4 spectra (or equivalently the NESR, which is similar). The calibration error, which actually could show some correlations over the frequencies, it is negligible with respect to the main statistical component.

Ref: Turner, D. D.: Arctic Mixed-Phase Cloud Properties from AERI Lidar Observations: Algorithm and Results from SHEBA, J. Appl. Meteorol., 44, 427–444, 2005.

9, 25-29 – It should be made more clear that all these LBLRTM-based regression approaches are being applied to the MIR observations and not the LBLRTM simulated radiances. ☑

10,11 – Using the mean difference may allow some cancellation of errors between the spectral points that are being averaged. It might be better to use the mean absolute value of the differences.

The absolute mean value of the differences is not much different from the mean difference since biases between extensions and the original observed spectra tend to follow trends in some spectral bands (positive between 300 and 550 cm-1 and negative between 170 and 300 cm-1) as seen in Figure 4 and 6.

Section 4

10,15 – “exhibited” would be better than “exemplified”. Also, “affect”, not “effect”. ☑

***11, Fig 6 – I think that the result that is plotted is from a single case. If so, please label it as such. However, if true, that opens up a more serious critique. Until the paper gets to Table 1, all results shown and discussed are from an example, not from the full dataset. How can the reader know whether these results are representative of the entire dataset?**

Results in figure 6 are not related to a single case, but using the entire set together (as well as in figure 4b). Only figures 1, 3 and 4a are related to a specific case as examples.

***12,9-15 – This section is puzzling. It is not up to a user’s discretion whether to interpret the relative humidity measured by a sonde as being with respect to liquid or ice saturation pressure. This is determined by the sonde design and processing software, and is done with respect to liquid. Interpreting it with respect to ice is not correct. In addition, it is difficult to understand the logic behind the statement in lines 13-15 “(indirectly implies : : :”). Why would changing the poor results obtained from sonde water vapor profiles obtained by the method described in this paragraph have anything to do with applying the methods in this paper to other conditions? This entire paragraph should be deleted.**

Actually, this paragraph was deleted from a previous draft of the article which was not submitted. As seen online (and on the ACP editor board), the actual submitted paragraph at page 12 between lines 9 to 15 is related to studies on the impact of the chimney.

12,21 – Perhaps add a few words to clarify: “: : : the vertical resolution and assumptions made in our modelling approach without adding a chimney layer are sufficient : : :”

We performed tests on the difference between observations and simulated spectra assuming the first level being outside the chimney and the first level being inside the chimney. The difference between both cases appears to be lower than 0.1 r.u. (below 600 cm^{-1}) and peaking at 0.2 r.u. in the centre of the CO_2 band (as seen on figure r6). This information has been added to the text.

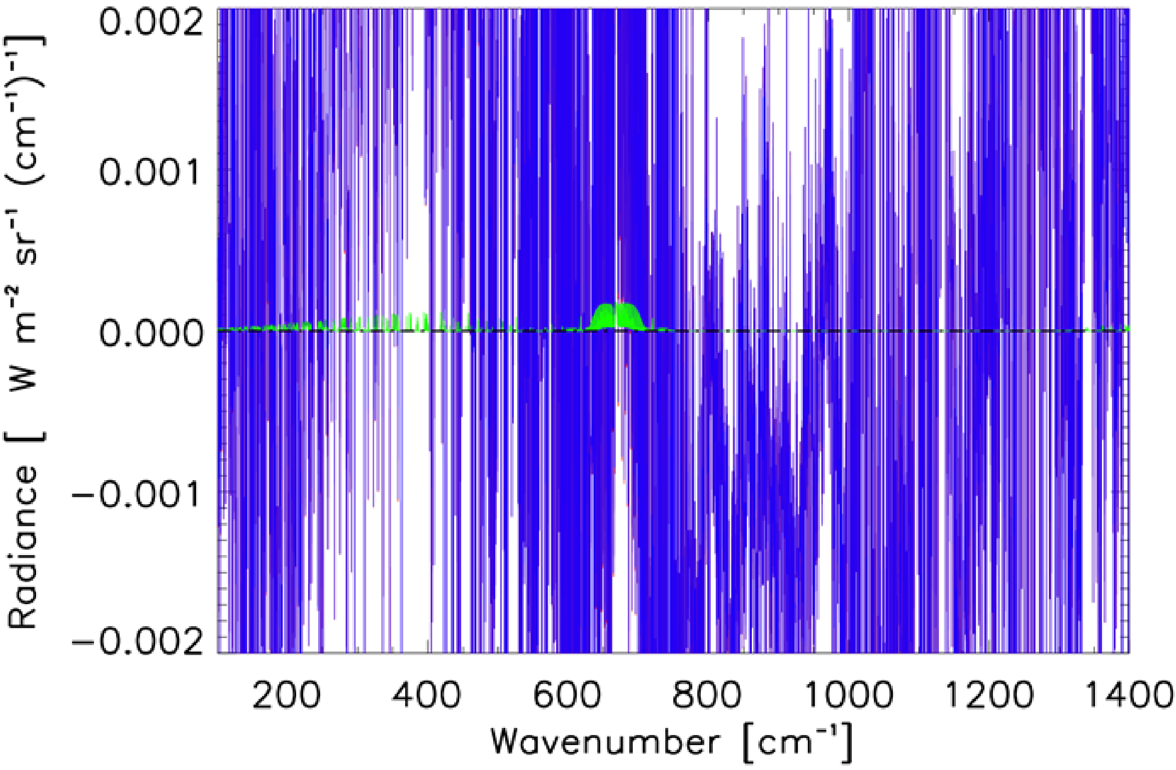

Figure r6: Blue: REFIR-PAD – LBLRTM using a first level from the chimney mean temperature from 2016. Red: REFIR-PAD – LBLRTM with our basic vertical resolution. The red curve is superposed below the blue curve. Green: LBLRTM with our basic vertical resolution – LBLRTM with the test first level.

Section 5

***14,1 – The Rizzi et al. paper certainly shows that current spectroscopy is sufficient to match observations and is an improvement over previous spectroscopy. The results in this paper show nothing of the kind. Perhaps the LBLRTM results the authors performed also indicate this. However, these results have not been presented in this manuscript.**

Indeed, the writing of the corresponding sentence tends to mislead the reader as we did not present in the article comparisons between REFIR-PAD data and the corresponding simulations (as seen in figure r7). The part of the sentence has been removed (taking into account the next point too).

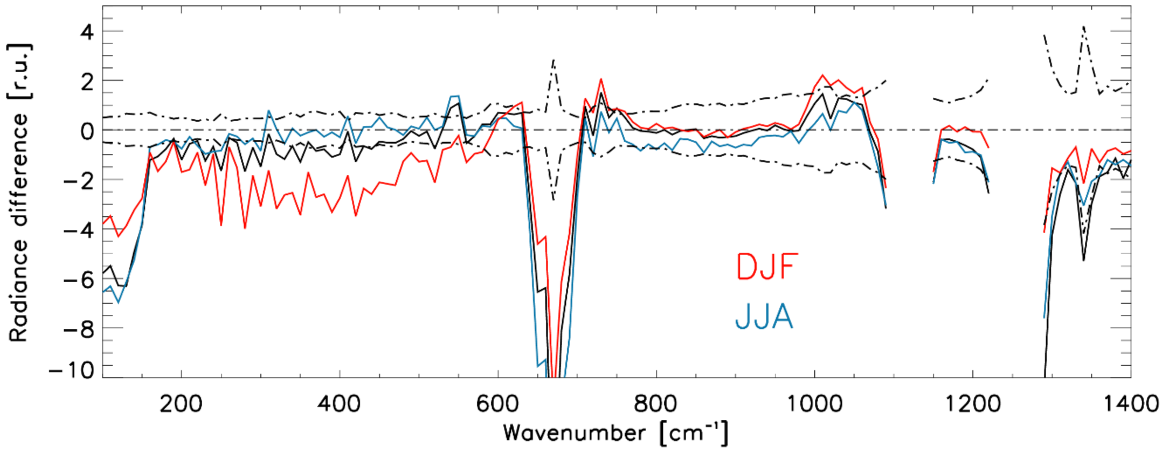

Figure r7: Mean radiance differences between REFIR-PAD and LBLRTM for the whole year (black), summer time (red) and winter time (blue).

***14,2-3 – The paper has not shown that an unbiased atmospheric state is essential to the approach that has been demonstrated. Water vapor profiles from sondes under very dry conditions are known to be biased (e.g. Miloshevich et al. (2009)), so the profiles that are used in this paper are likely far from unbiased.**

The relative humidity measurements have been corrected by the algorithms of Miloshevich et al. (2009) as explained in Tomasi et al. (2011):

For this purpose, use was made of (1) the lag error corrections estimated by Rowe et al. [2008] (R08 hereinafter) in the presence of strong temperature inversions near the ground at Dome C; (2) the algorithm of Cady-Pereira et al. [2008] (C08 hereinafter) for correcting the RS80-A solar heating dry biases affecting the relative humidity (RH) measurements, properly normalized to the dry bias estimates made by R08 at Dome C; and (3) the algorithms of Miloshevich et al. [2009] (M09 hereinafter) for correcting the RS92 instrumental errors affecting RH. Using these algorithms, more reliable evaluations of RH have been obtained than those achieved by T06 in April–May 2005.

In addition, although we did not show it in the article, we changed and tested various RH profiles to assess the extension, with large biases seen.

***14,13-15 – As in the comment above, this really has not been shown. At best, the analysis about the water vapor saturation pressure over ice that is alluded to (but not really shown) suggests that this might be true, but this is far from being demonstrated.**

This part was also in a previous draft of the manuscript and was not discussed in the submitted version.

14,24-29 – It is unclear what the results from this ground-based study have to do with the possible future FORUM mission. The authors should make their argument here more clearly or abandon it.

The possible future FORUM mission aims to provide the first FIR global data set observed from space (along with MIR data). T15 suggests that is it possible to extend MIR to FIR using a predictor model. However, this model has been built using LBLRTM simulations and has only been compared to broadband observations. Using the REFIR-PAD observations, we observe that such an approach can achieve acceptable accuracy if instrument noise is taken into account. Therefore, it seems feasible that a model to extend the MIR to the FIR as described by T15 could be built using FORUM data. This model would need to be assessed by the FORUM measurements as we have done here with REFIR-PAD data. If successful, such a model could be used retrospectively on IASI (after collocated verifications between IASI extensions and FORUM) to estimate long trends of FIR radiances for use in, say, model evaluation. Note that of course we are not saying that the regression model we have built here is suitable for this purpose, simply that the technique appears viable.

Can downwelling far-infrared radiances over Antarctica be estimated from mid-infrared information?

Christophe Bellisario[1], Helen E. Brindley[2], Simon F.B. Tett[1], Rolando Rizzi[3], Gianluca Di Natale[4], Luca Palchetti[4], and Giovanni Bianchini[4]

[1]School of Geosciences, University of Edinburgh, Crew Building, The King's Buildings, Edinburgh EH9 3FF, UK
[2]Space and Atmospheric Physics Group, National Centre for Earth Observation, Imperial College London, London, UK
[3]Department of Physics and Astronomy, University of Bologna, Bologna, Italy
[4]Istituto Nazionale di Ottica - CNR, Sesto Fiorentino, Italy

Correspondence: Christophe Bellisario (christophe.bellisario@ed.ac.uk)

Abstract. Far-infrared (FIR: 100 $\mathrm{cm^{-1}}$ < wavenumber, ν < 667 $\mathrm{cm^{-1}}$) radiation emitted by the Earth and its atmosphere plays a key role in the Earth's energy budget. However, because of a lack of spectrally resolved measurements, radiation schemes in climate models suffer from a lack of constraint across this spectral range. Exploiting a method developed to estimate upwelling far-infrared radiation from mid-infrared (MIR: 667 $\mathrm{cm^{-1}}$ < ν < 1400 $\mathrm{cm^{-1}}$) observations, we explore the possibility of inferring zenith FIR downwelling radiances in zenith-looking observation geometry, focusing on clear-sky conditions in Antarctica. The methodology selects a MIR predictor wavenumber for each FIR wavenumber based on the maximum correlation seen between the different spectral ranges. Observations from the REFIR-PAD instrument (Radiation Explorer in the Far Infrared - Prototype for Application and Development) and high resolution radiance simulations generated from co-located radio soundings are used to develop and assess the method. We highlight the impact of noise on the correlation between MIR and FIR radiances by comparing the observational and theoretical cases. Using the observed values in isolation, between 150 and 360 $\mathrm{cm^{-1}}$, differences between the 'true' and 'extended' radiances are less than 5 %. However, in spectral bands of low signal, between 360 and 667 $\mathrm{cm^{-1}}$, the impact of instrument noise is strong and increases the differences seen. When the extension of the observed spectra is performed using regression coefficients based on noise-free radiative-transfer simulations the results show strong biases, exceeding 100 % where the signal is low. These biases are reduced to just a few percent if the noise in the observations is accounted for the simulation procedure. Our results imply that while it is feasible to use this type of approach to extend mid infrared spectral measurements to the far-infrared, the quality of the extension will be strongly dependent on the noise characteristics of the observations. A good knowledge of the atmospheric state associated with the measurements is also required in order to build a representative regression model.

1 Introduction

Defined here as wavelengths above 15 μm or wavenumbers below 667 $\mathrm{cm^{-1}}$, the far-infrared (FIR) spectral band plays a key role in energetic exchanges between the Earth's surface, atmosphere and space (Harries et al., 2008). Under clear-sky conditions, absorption in the FIR is dominated by water vapour such that typically very little FIR radiation emitted from the surface directly escapes to space. However, the very cold, dry conditions commonly found in polar regions simultaneously shift the peak of surface emission towards longer wavelengths and, under clear-skies, allow as much as 45 % of FIR radiation emitted from the ground to escape directly to space, making the clear-sky FIR outgoing longwave radiation sensitive to surface properties (Feldman et al., 2014). A corollary of this enhanced atmospheric transmissivity is the increased sensitivity of downward clear-sky FIR radiation at the surface to conditions at higher levels in the atmosphere than would normally be the case in warmer, wetter environments.

Despite its role in the energy budget, due to the inherent difficulties involved, only a few instruments have measured hyper-spectral radiances across the FIR. Aircraft and ground based measurements available from the Tropospheric Airborne Fourier Transform Spectrometer (TAFTS) (Canas et al., 1997) have been used to probe water vapour spectroscopy; upper tropospheric humidity; the radiative properties of cirrus and snow/ice surface emissivity (Green et al., 2012; Fox et al., 2015; Cox et al., 2007; Cox et al., 2010; Bellisario et al., 2017). Balloon and ground-based observations from the Radiation Explorer in the Far InfraRed - Prototype of Applications and Development (REFIR-PAD, Bianchini et al., 2006) have been exploited to determine precipitable water (Bianchini et al., 2011), investigate the spectral signature of cirrus (Maestri et al., 2014) and provide simultaneous retrievals of water vapour, temperature and cirrus properties (Di Natale et al., 2017). The Far-InfraRed Spectroscopy of the Troposphere (FIRST) instrument (Mlynczak et al., 2006) has participated in both balloon and ground-based campaigns, providing a rigorous test of the ability of radiative transfer models to match the spectroscopic signals measured in the far infrared (Mlynczak et al., 2016; Mast et al., 2017). All three of these instruments participated in one or both the Radiative Heating in Underexplored Bands Campaigns (RHUBC), providing a robust dataset which has been used to improve our knowledge of the underlying far-infrared water vapour spectroscopy (Turner and Mlawer, 2010).

Almost all of the available FIR radiance measurements originate from limited field campaigns. Recognising the key role that the FIR plays in determining the Earth's energy budget, the information that may be contained in the spectrum, and the lack of available measurements, Turner et al. (2015, hereafter T15) describe a methodology designed to estimate FIR radiances by exploiting correlated behaviour in the MIR. They applied this method to nadir radiance measurements from the Infrared Atmospheric Sounding Interferometer (IASI, Clerbaux et al., 2009) and evaluated their approach by comparing spectrally integrated radiances across the infrared with measurements from the Clouds and the Earth's Radiant Energy System (CERES, Wielicki et al., 1996) broadband radiometers taken during simultaneous nadir overpasses. Overall mean broadband agreement is encouraging but the evaluation technique precludes the identification of any compensating biases within the FIR itself. In essence, the T15 methodology, and similar methods that seek to create synthetic FIR top-of-atmosphere spectra from mid-infrared observations (e.g. Huang et al., 2008) have not been evaluated with real spectral observations due to the absence of such measurements. As shown by Huang et al. (2008, 2013), estimates of spectrally resolved fluxes across the infrared can provide a powerful tool for climate model evaluation.

REFIR-PAD has been measuring spectral downwelling longwave radiances at Dome-C Antarctica since 2011, providing a long-term database covering the spectral range from 100 to 1400 cm^{-1} (Palchetti et al., 2015). In this study we exploit the availability of these observations to test whether a similar methodology to that described by T15 can be developed and applied to the REFIR-PAD measurements. Unlike T15, our goal is not to create an algorithm that can be applied on the global scale but simply to evaluate the performance of such an approach under the very specific conditions sampled by REFIR-PAD during its deployment. We focus on clear-sky conditions, essentially providing a test of the unique information contained in the FIR relating to water vapour spectroscopy and concentration. Because spectrally resolved observations covering much of the infrared are available, inferred FIR spectral radiances can be compared to the real observations, providing a thorough evaluation of the success of the technique. Radiative transfer simulations utilising radiosonde measurements of the atmospheric state can also be used to assess the impact of instrumental and sampling noise on the robustness of the relationships seen. In this way we are able to assess to what level it is possible to use information in the MIR (within the constraint of the REFIR-PAD wavenumber range and location) to infer FIR spectral behaviour using actual observations.

Given the constrained nature of the REFIR-PAD dataset, if the results show that the approach fails to capture the observed spectral behaviour it would cast serious doubt on whether our ability to model the full infrared spectrum is sufficient for us to expect a similar approach to give a robust spectral prediction over a wider range of conditions and/or viewing geometries. Conversely, while a successful implementation does not directly imply that a similar level of agreement will be seen in other locations and for other viewing geometries, it does give confidence that the general principle is robust.

In section 2, the instrumental data are described along with the radiative transfer model used to produce simulated spectra for comparisons. We also describe the distinct steps of the spectral extension method. Section 3 displays the results, with comparison between instrumental and theoretical extensions, which are discussed in section 4. We also investigate the impact of spectral averaging, consistent with the type of resolution currently employed in global climate models as a key potential use of such data are for model evaluation. Finally we draw conclusions in section 5.

2 Data and methodolgy

2.1 REFIR-PAD

The REFIR-PAD instrument is currently located at the Italian-French Concordia research station in Antarctica (75°06'S, 123°23'E) at 3,230 m above sea level. It was installed in the Physics Shelter, south of the main station buildings for the PRANA project (Proprietà Radiative dell'Atmosfera e delle Nubi in Antartide), financed by the Italian PNRA (Programma Nazionale di Ricerche in Antartide). The PRANA project aimed to supply the first multi-year dataset of spectral downwelling longwave radiances, including the unique measurements in the FIR over a polar region, and the instrument has been recording data autonomously since 2011 (Palchetti et al., 2015) with further support from projects CoMPASS (COncordia Multi-Process Atmospheric StudieS), the currently active DoCTOR (DOme C Tropospheric ObserveR) and FIRCLOUDS (Far Infrared Radiative Closure Experiment For Antarctic Clouds). A protective chimney separates the instrument from the outside temperature and the ingress of wind and snow is prevented by a barrier on the rooftop.

The instrument, fully described in Bianchini et al. (2006), is composed of a Fourier transform spectroradiometer (Mach-Zehnder type) with an operating spectral bandwidth of 100 - 1400 cm^{-1} (100 - 7.1 μm) at a resolution of 0.4 cm^{-1} and with an acquisition time of 80 s. One calibrated spectrum is based on the average of four zenith observations for an overall measurement time of 6.5 min every 14 min. The noise equivalent spectral radiance (NESR) due to detector noise is approximately 1 mW m^{-2} sr^{-1} (cm^{-1})$^{-1}$ at 400 cm^{-1}. In addition to the radiometric NESR, the calibration error and the standard deviation of the four observations composing the calibrated spectrum are calculated. The standard deviation is a posteriori estimation that includes the NESR and possible scene variations (Palchetti et al., 2015).

The selection of the clear-sky spectra uses the classification outlined in Rizzi et al. (2016) to discriminate between clear and cloudy scenes for 2013. Twenty-four spectral intervals are selected and seven tests are applied, comparing the mean radiances, the standard deviation and the brightness temperature in the specified spectral intervals. This approach yields 5126 clear sky spectra for 2013.

We choose to focus only on clear-sky conditions because this gives us a reasonably well-constrained dataset to use in testing the extension approach. Including cloudy conditions would require a successful detection of cloud-type, height and microphysics to incorporate into the radiative transfer modelling described in section 2.3, adding significant complexity to the study. From previous theoretical studies and ongoing work analysing the REFIR-PAD spectra, we also expect unique information related to ice crystal habit to be contained within the FIR micro-windows (Yang et al., 2003; Maestri et al., 2014; Di Natale et al., 2017).

An example of a clear-sky spectrum is displayed in figure 1 and shows unphysically high radiances and standard deviations in two bands within the atmospheric window region, from 1095 - 1140 cm^{-1} and 1230 - 1285 cm^{-1}. These are a manifestation of absorption by the polyethylene terephthalate (Mylar) substrate which composes the wideband beam splitter and hence radiances within these bands are not used in this study. Outside these two regions and where the downwelling signal is typically high (below 400 cm^{-1} and between 600 and 800 cm^{-1}), the standard deviations are relatively small. However, in the most transparent regions, where the radiance is low (micro-windows between 400 - 600 cm^{-1} and in the atmospheric window from 800 - 1000 cm^{-1} for example), the standard deviations can exceed the measured radiances with values around 2 r.u. (radiance unit), where 1 r.u. is equivalent to 1 mW m^{-2} sr^{-1} (cm^{-1})$^{-1}$.

2.2 Radiosonde profiles

Since 2005, the radiosonde system routinely operative at Dome C has provided atmospheric pressure, temperature and humidity profiles at 12 UTC. From 2009 onwards these observations have been made using the Vaisala RS-92SPGW. The daily profiles are available at www.climantartide.it.

During a radiosonde launch, data are recorded every 2 seconds, corresponding to around 800 measurements in the troposphere, and between 900 to 1900 measurements in the stratosphere, reaching up to 26-30 km (Tomasi et al., 2011). However, the relative humidity is only measured up to 15 km. Due to the balloon ascent rate (5-6 m s^{-1}) and the recording rate, the vertical resolution is about 10-12 m. Raw water vapour profiles are provided in relative humidity and the conversion to mixing ratio assumes saturation over water as advised by the World Meteorological Organisation (WMO) guide to meteorological instruments and methods of observation (https://www.wmo.int/pages/prog/www/IMOP/CIMO-Guide.html).

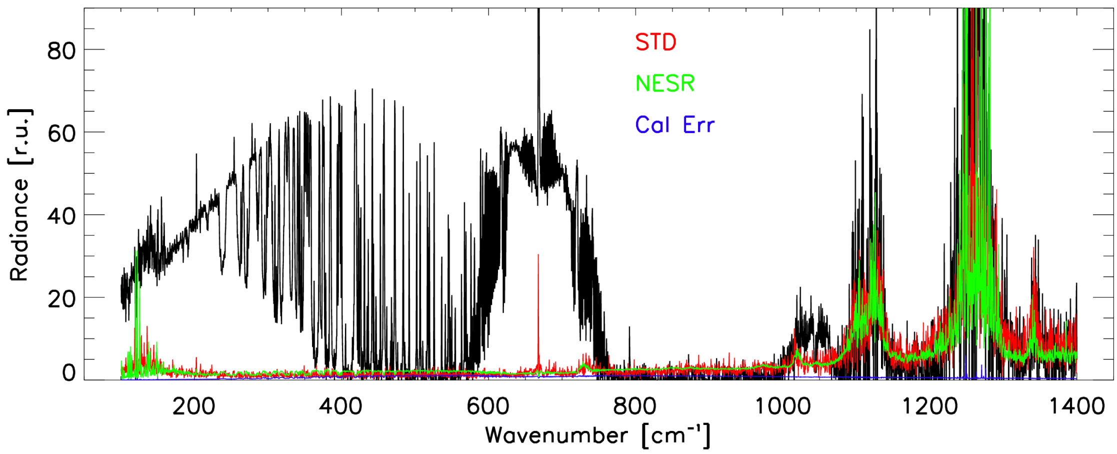

Figure 1. Example of a clear-sky spectrum as seen from REFIR-PAD in black, and its associated standard deviation (in red), the noise equivalent spectral radiance (in green) and the calibration error (in blue).

2.3 LBLRTM

We use the Line-By-Line Radiative Transfer Model (LBLRTM, Clough et al., 2005) to simulate the downwelling radiance. The version used in this study is LBLRTM v12.7, with an updated line parameter database AER version 3.5 (following HITRAN 2012, Rothman et al. (2013)) and a continuum code MT_CKD_3.0 which an includes up-to-date representation of the H_2O foreign continuum from 0-600 cm^{-1} and of the self continuum in the microwave that resulted from an analysis of measurements taken at the ARM RHUBC-II campaign and a re-analysis of RHUBC-I measurements (not included in T15).

The radiosonde profiles described in section 2.2 provide the temperature and water vapour inputs for the radiative transfer simulations. The radiosonde profiles are interpolated onto 100 levels, with the highest vertical resolution being 26 m near the surface. Additional levels extending up to 50 km in altitude are included using temperature and humidity data from the closest ERA-Interim (Dee et al., 2011) profiles in space and time, scaled to the highest altitude where reliable temperature and water vapour values were recorded by the given radiosonde. Ozone concentrations are extracted from the same ERA-Interim profile. Minor species are taken from the AFGL sub-Arctic winter and summer profiles (Anderson, 1986) and CO_2 has been scaled to 2013 values as reported by NOAA's Global Monitoring Division, Earth System Research Laboratory (https://www.esrl.noaa.gov/gmd/ccgg/trends/). To achieve consistency with the REFIR-PAD instrumental characteristics, each simulated spectrum is Fourier transformed and a maximum optical path difference of 1.25 cm is applied in the interferogram domain. The truncated interferogram is then re-transformed and the resulting spectrum is sampled at the REFIR-PAD sampling frequency.

2.4 Extension methodology

Based on the methodology developed by T15, FIR wavenumbers between 100 and 667 cm^{-1} are correlated with (predictor) wavenumbers from 667 to 1400 cm^{-1}. The estimated radiance in the FIR $I_{\nu,FIR}$ can be written as a function of the predictor radiance $I_{\nu,predictor}$, and two regression coefficients, a_0 and a_1, using:

$$\ln(I_{\nu,FIR}) = a_0 + a_1 \ln(I_{\nu,predictor}) \tag{1}$$

given the assumption of a logarithmic relationship between the predictor and estimated radiances and

$$I_{\nu,FIR} = a_0 + a_1 I_{\nu,predictor} \tag{2}$$

for a linear assumption.

We start by selecting the REFIR-PAD spectra that will be used to calculate the regression coefficients. All clear-sky spectra that are closest in time to the daily radiosonde measurement at 12 UTC are selected. If the closest spectrum on a given day is measured more than two hours before or after 12 UTC, the spectrum is discarded. 125 days during 2013 are retained using this criterion. These spectra are randomly divided into two sets. The first set is used as a creation set, from which the regression coefficients are derived and the second is used as a test set, on which the regression coefficients derived from the creation set are tested.

To choose the predictor wavenumbers, we select a FIR wavenumber and create a vector composed of all radiances in the creation set at this wavenumber. We compute the correlation of this vector with a similar vector at a MIR wavenumber. We repeat this analysis for all MIR wavenumbers and select the MIR wavenumber that shows the highest correlation as the predictor for the given FIR wavenumber. Finally, the linear (or logarithmic) regression coefficients are calculated. The whole process is repeated for each FIR wavenumber. We emphasize that the methodology described here is only based on analytical considerations with the computation of the correlation. No spectral assumptions are made and as a consequence the MIR predictor wavenumbers can be associated either with, for example, a CO_2 line, a H_2O line or a combination of both.

3 Results

3.1 Application to observed spectra

Figure 2(a) displays the correlation between FIR and MIR radiances using the REFIR-PAD creation set, displayed at the nominal instrument spectral resolution of 0.4 cm^{-1}. As noted previously, the bands corresponding to regions of high noise due to the absorption by the beam-splitter (1095 - 1140 cm^{-1} and 1230 - 1285 cm^{-1}) have been removed from the analysis.

We observe specific spectral regions that maximise the correlation. A large portion of the spectral region between 150 and 500 cm^{-1} is highly correlated with wavenumbers between 667 and 720 cm^{-1}. Figure 2(b) indicates the MIR predictor wavenumber selected for each FIR wavenumber using the approach described in section 2.4. Below 150 cm^{-1}, the predictor wavenumbers are scattered between 700 and 1400 cm^{-1} with low correlation values, between 0.2 and 0.5. This can be explained

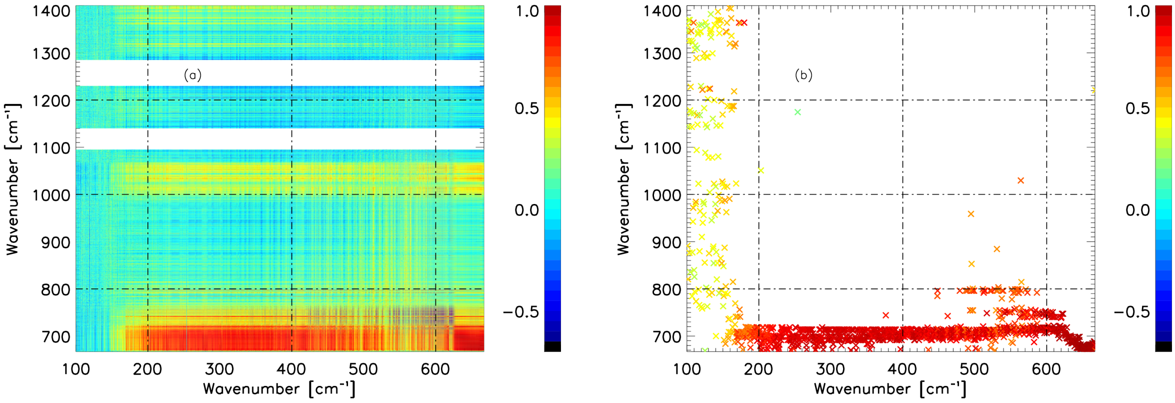

Figure 2. (a) Correlation map using REFIR-PAD clear-sky spectral radiances with MIR wavenumbers on the y axis and FIR wavenumbers on the x axis. (b) MIR wavenumbers that maximise the correlation for each FIR wavenumber. Colour scales indicate the correlation.

by a high NESR at the edge of the REFIR-PAD detector as seen in figure 1 in green. Between 200 and 470 cm^{-1}, the predictor wavenumbers are clustered around 700 cm^{-1}, within the wing of the 667 cm^{-1} CO_2 band, with correlations of between 0.84 and 0.94. Figure 2(a) shows lower, more varied correlations in the 470 and 570 cm^{-1} region: here the MIR predictor wavenumber also shows more variability taking values varying between 696 and 799 cm^{-1}. The correlation values in this region lie between 0.71 and 0.92. Moving towards the centre of the 667 cm^{-1} CO_2 band, MIR predictors are typically clustered at 682 cm^{-1} and show a narrower range of higher correlations of between 0.96 and 0.98. We note that the predictor wavenumbers are mainly localised in a spectral area dominated by the CO_2 band coexisting with typically weaker vapour lines.

As noted in section 2.4, regression coefficients a_0 and a_1 in equations 1 and 2 are computed between each FIR wavenumber and the corresponding predictor MIR wavenumber. Figure 3 shows an example of the relationship between a predictor wavenumber at 698.4 cm^{-1} and its corresponding predictand wavenumber at 301.6 cm^{-1} across all creation set spectra. Logarithmic (Eqn 1) and linear (Eqn 2) fits between the radiances are also displayed.

Using the test set of spectra we examined the robustness of the extension method. An example of a single REFIR-PAD observation (in black) and its extension (in blue) is displayed in figure 4(a) with the radiance and relative differences in figure 4(b) at 10 cm^{-1} resolution. In this case, linear regressions have been used to perform all the extensions. Displaying the results at 10 cm^{-1} allows a clearer picture to emerge in terms of the performance of the extension.

At 10 cm^{-1} resolution the mean absolute standard deviation across the FIR over the entire test set is relatively small at less than 0.6 r.u. It is worth nothing that below 370 cm^{-1} the mean error fluctuates around zero but at higher wavenumbers (370 cm^{-1} $< \nu <$ 600 cm^{-1}) there does appear to be a small positive bias of $\sim$ 0.5 r.u. Under clear-sky conditions this region is generally more transmissive than the lower wavenumber regime - as evidenced by the comparatively lower radiances in figure 4(a). These lower radiances, particularly between 400 and 570 cm^{-1}, contribute to slightly higher relative differences and variability across this range in figure 4(b). Above 570 cm^{-1}, both absolute and relative differences diminish as the radiance increases.

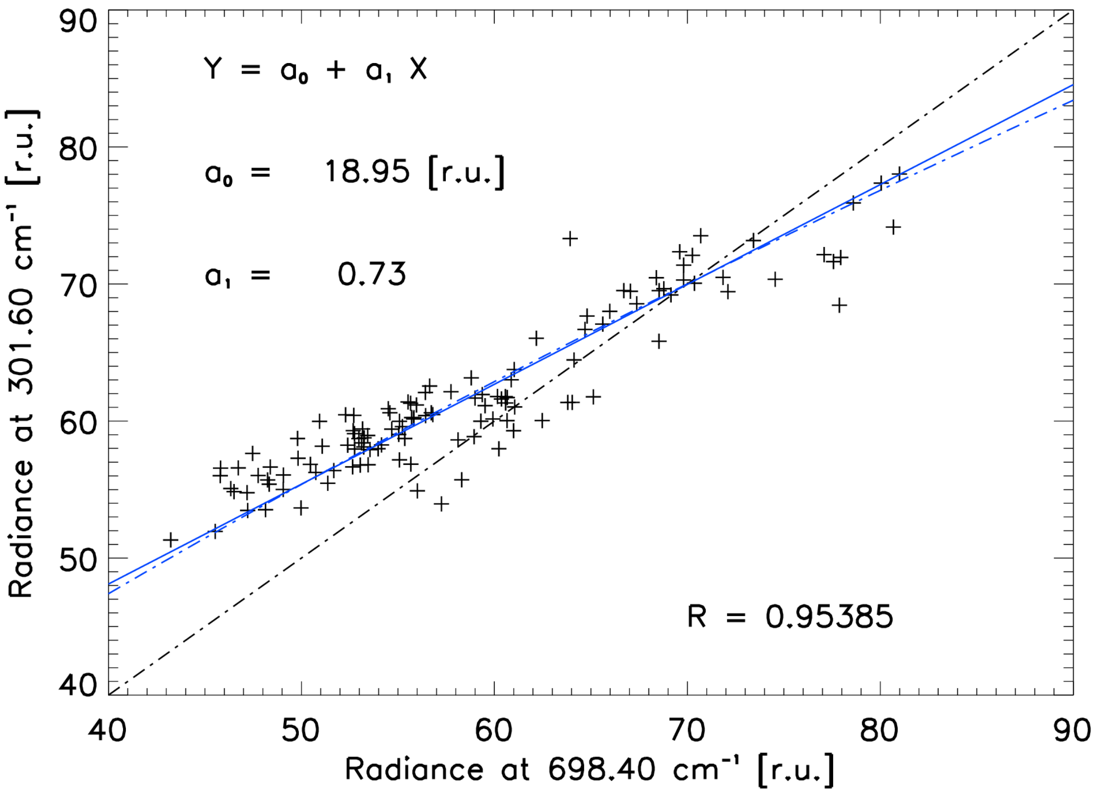

Figure 3. FIR radiances at 301.6 cm^{-1} against predictor MIR radiance at 698.4 cm^{-1} for all creation set spectra. The solid blue line is the linear fit of the points using equation 2, with regression coefficients a_0 and a_1. The linear correlation value R is indicated. For completeness, the logarithmic fit is also shown by the dashed blue line. The black dash-dotted line represents 1:1.

3.2 Application to simulated spectra

The previous section suggests that a reasonable reconstruction of observed clear-sky downwelling FIR surface spectral radiances at a moderate (10 cm^{-1}) resolution can be obtained using simultaneous observations of MIR radiances. In this section we explore whether similar results are obtained using simulations.

Therefore, we apply the same process of extension using simulated LBLRTM spectra. For each clear-sky case used to build the creation and test sets for REFIR-PAD data, the corresponding radiosonde profile is selected and used as input for LBLRTM as described in section 2.2. The output spectra are used to generate the equivalent simulated creation and test sets.

We consider two cases. The first uses the LBLRTM spectra as directly simulated, while the second adds noise in order to be more representative of the REFIR-PAD observations. Noise is introduced using the following equation:

$$I'_{\nu,LBLRTM} = I_{\nu,LBLRTM} + r * MAX\left(\sigma_{\nu,REFIR-PAD}, \sqrt{NESR^2_{\nu,REFIR-PAD} + CalErr^2_{\nu,REFIR-PAD}}\right) \quad (3)$$

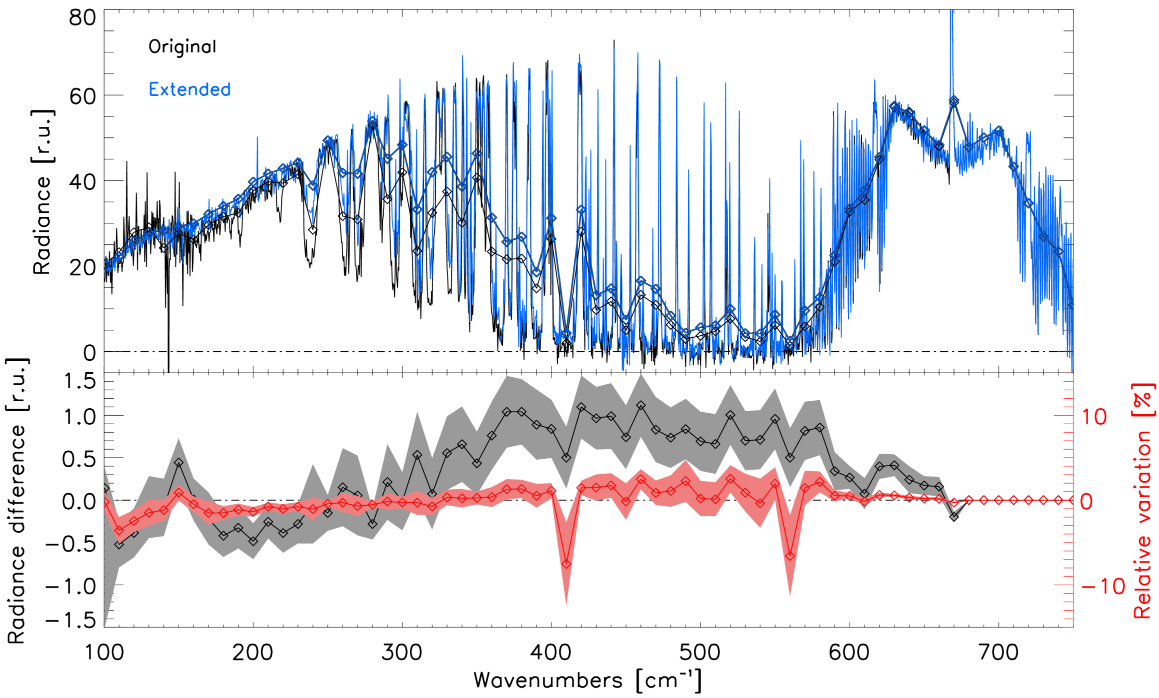

Figure 4. Far-infrared extension based on REFIR-PAD data (linear case). (a) Example of a spectrum (black) and its extension (blue) below 667 cm^{-1}. The same spectra integrated over 10 cm^{-1} bands are also shown by the diamond lines. (b) Mean difference (black) and relative variation (red) between the original and the extended spectra at 10 cm^{-1} resolution calculated over the entire test set. Shaded areas are the associated standard deviations.

where $I'_{\nu,LBLRTM}$ is the spectral radiance from LBLRTM with noise, $I_{\nu,LBLRTM}$ is the 'noise-free' spectral radiance directly simulated by LBLRTM, r is a normally distributed random number between -1 and 1 and $\sigma_{\nu,REFIR-PAD}$, $\mathrm{NESR}_{\nu,REFIR-PAD}$ and $\mathrm{CalErr}_{\nu,REFIR-PAD}$ are respectively the standard deviation, the Noise Equivalent Spectral Radiance and the Calibration Error from the corresponding REFIR-PAD spectrum.

The correlation maps of LBLRTM with and without noise are displayed in figures 5(a) and 5(b) respectively. Taking the no-noise case first, most wavenumbers show a strong correlation with all others, with values typically above 0.5. The FIR band sees an enhanced correlation with the MIR between 667-950 cm^{-1} and wavenumbers between 1300 and 1400 cm^{-1}. When noise is added, the correlations reduce and show a much greater spectral variation which is more consistent with the observational case. The same bands seen in figure 2(a) which maximise the correlation appear.

The predictor wavenumbers are displayed in figure 5 without noise (c) and with noise (d). In the case of a perfect simulation, the number of predictor wavenumbers is relatively small, indicating a high degree of correlation in the spectra. Below 600 cm^{-1}, most of the predictor wavenumbers are located between 1340 and 1400 cm^{-1}. As a comparison, T15 find predictor wavenumbers outside the REFIR-PAD spectral range, between 1500 cm^{-1} and 1600 cm^{-1} towards the centre of the ν_2 water

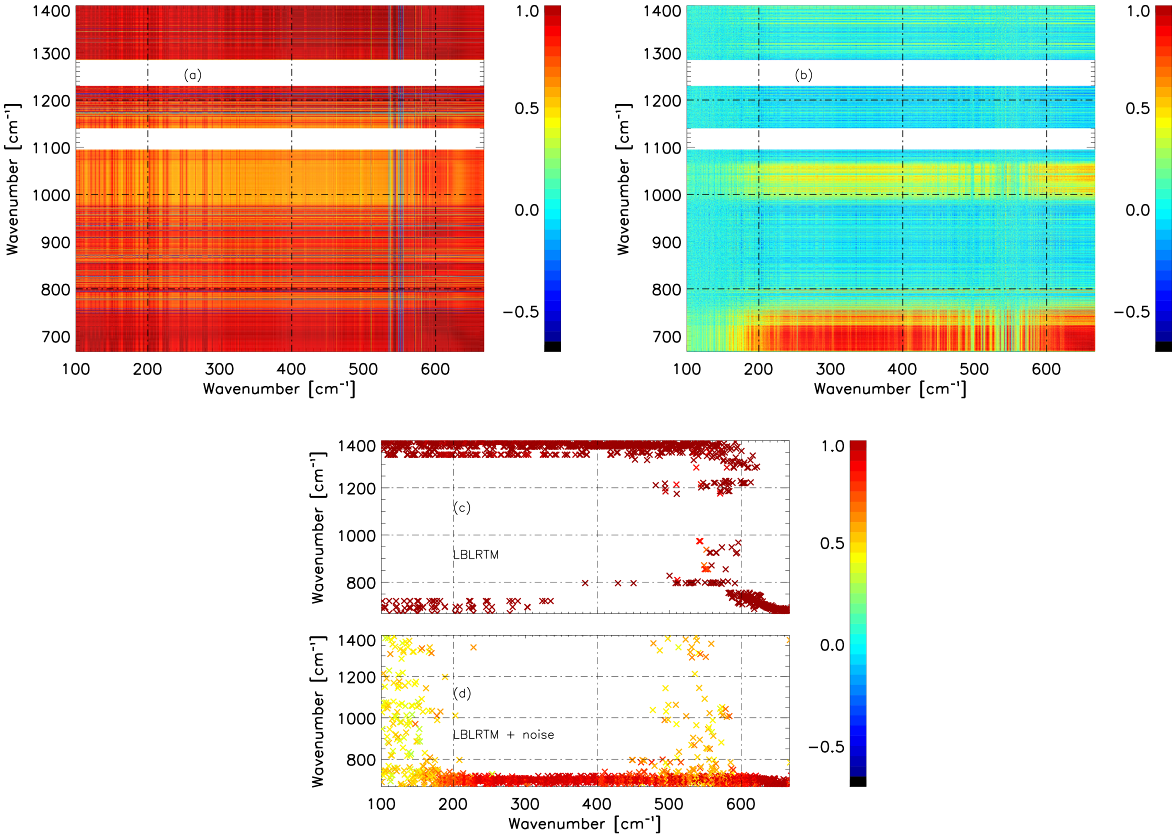

Figure 5. Correlation map using noiseless LBLRTM spectra (a) and LBLRTM spectra with realistic noise added (b). (c) and (d) As figure 2(b) showing predictor wavenumbers for LBLRTM without noise and with noise respectively.

vapour vibration-rotation band. Below 300 cm^{-1}, a second band is visible around 700 cm^{-1}. Between 600 and 667 cm^{-1}, the predictor wavenumbers are spread over a range of discrete values close to 700 cm^{-1}. When the LBLRTM simulations are perturbed with noise, consistent with the change in the correlation map, the selected predictor channels show similar behaviour to REFIR-PAD (figure 2(b)). Below 160 cm^{-1}, the predictor wavenumbers are located in a wide band between 667 and 1400 cm^{-1}, but with a correlation of about 0.5. Between 200 and 400 cm^{-1}, the predictor wavenumbers are distributed in a band centred at 700 cm^{-1}. Above 400 cm^{-1}, predictor wavenumbers up to 800 cm^{-1} also begin to appear while between 500 and 600 cm^{-1} the spread in predictors again extends across the whole 667 - 1400 cm^{-1} range with typically lower correlations.

At the time of writing there are only very limited spectrally resolved data in the FIR. The goal of this research is thus to see whether the LBLRTM simulations are able to provide coefficients to correctly map the observed MIR data into the FIR. So we now test the accuracy of going from observed MIR to FIR radiances using 3 different approaches. All predictions are then compared against the REFIR-PAD FIR observations. The 3 different sets of regression coefficients we use are:

– LBLRTM simulations (LBL),

– LBLRTM simulations + realistic noise (LBN),

– Coupled LBLRTM (LBC) where predictor wavenumbers are generated from LBLRTM + realistic noise but regression coefficients are generated from LBLRTM without noise.

By coupling the predictor wavenumbers from LBLRTM + noise and the regression coefficients from LBLRTM without noise in the last approach, we obtain the best estimate of regression coefficients at the wavenumbers where the expected relationship is strongest.

In all cases shown a linear regression is used although the findings are essentially unchanged if a logarithmic fit is employed (see table 1). Figure 6 displays the mean differences (a) and mean relative variations (b) between the 'true' and extended FIR radiances for all cases, with their associated standard deviations. For ease of comparison, the extension of REFIR-PAD based on REFIR-PAD derived regression coefficients (previously shown in figure 4(b)) is also included. The extension to the FIR using regression coefficients based on noise-free simulations (LBL) fails to capture the observed FIR behaviour. A strong bias is visible with a mean difference of -45 %. In this case, the selected predictor wavenumbers are close to 1400 $\mathrm{cm^{-1}}$ (figure 5(c)), however, at these wavenumbers, the observed correlation for REFIR-PAD is very low (figure 2(a)), due to increased noise (figure 1), leading to large differences between the extended spectra and observations. If the predictor wavenumbers are selected from the noise adjusted simulations (LBN and LBC), the mean differences and s show a marked decrease, reducing the mean difference to 1.1 % and -0.4 % for LBN and LBC respectively.

4 Discussion

Noise-free simulations of downwelling spectrally resolved clear-sky radiances over Antarctica imply a high level of correlation between the MIR and FIR. However, the prediction model based on these simulations fails to adequately capture observed behaviour under clear-skies as exhibited by REFIR-PAD. Instrumental noise characteristics strongly affect the choice of predictor wavenumbers. Including the effects of this noise in the simulations markedly improves the prediction model, which is capable of capturing the observed mean radiance in the FIR to within 2 %, except in selected bands where the downwelling radiance is low (for example 410 $\mathrm{cm^{-1}}$, 490 $\mathrm{cm^{-1}}$, with a peak at 540 $\mathrm{cm^{-1}}$, see figures 6(a) and (b)).

More specific to this study, it is worth noting that the temperature and water vapour profiles very close to the ground (within 2 m) may also be affected by the presence of the chimney connecting the physics shelter to the outside environment. Palchetti et al. (2015) perform a least squares minimisation of the radiance differences between the observation and the simulation, with the addition of a first level inside the chimney into the fitted profiles. Rizzi et al. (2016) include a first level inside the chimney based on the average between the internal PAD temperature and the shelter temperature. We performed tests on the first profile level in our simulations, adding a temperature point corresponding to the chimney mean temperature (of available year 2016). The differences between our vertical resolution and this test showed differences up to 0.2 r.u., peaking in the centre of the CO_2 band. In the absence of measurements of temperature inside the chimney for 2013 and bearing in mind the limited sensitivity

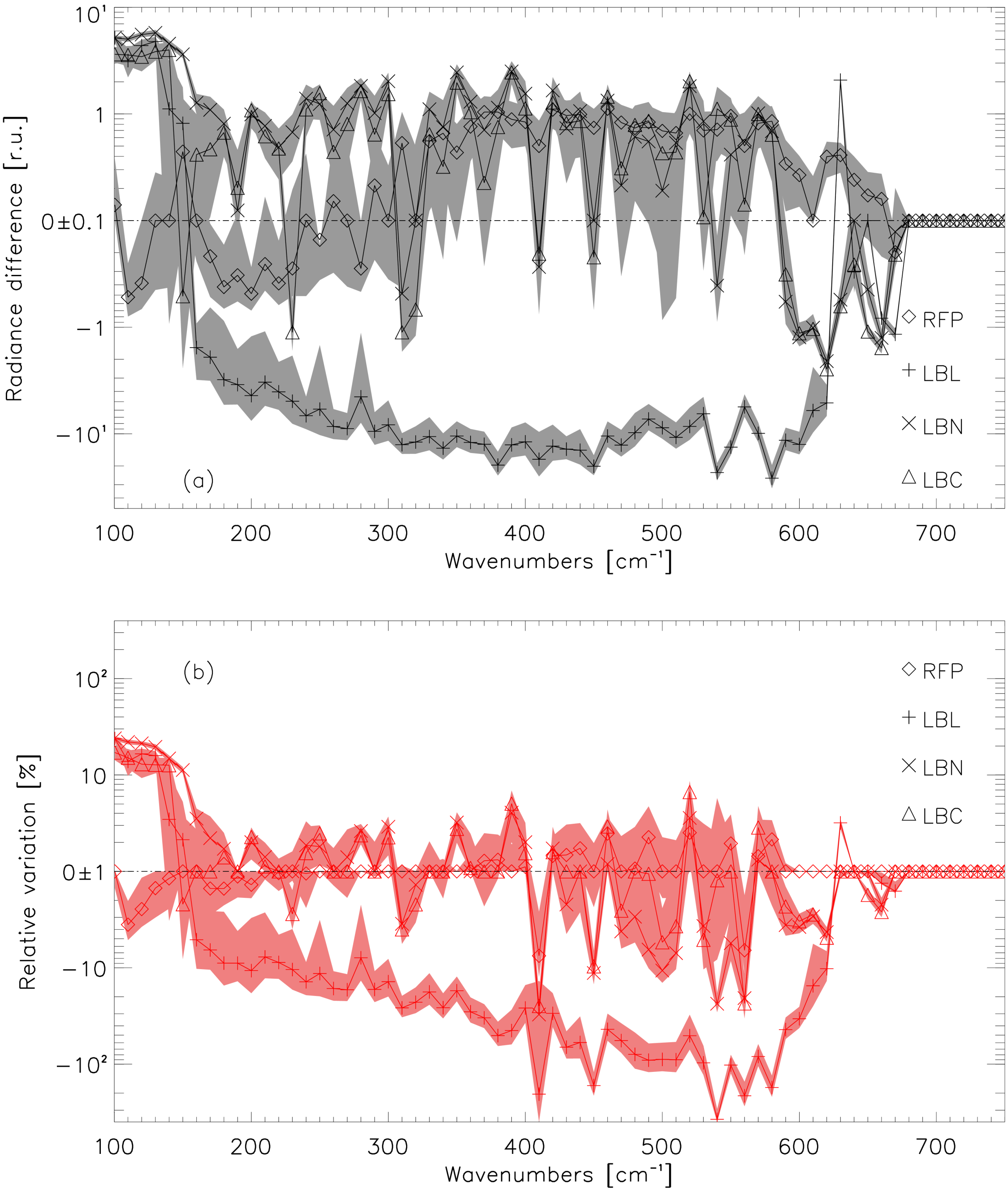

Figure 6. As figure 4(b) for all cases of linear extension, with (a) the radiance difference and (b) the relative variation, using $\diamond$ for REFIR-PAD (RFP), $+$ for LBLRTM (LBL), x for LBLRTM with noise (LBN), Δ for coupled LBLRTM (LBC).

Table 1. Distribution of the differences and relative variations between the extension and the original spectra within the three bands (100.4 - 400, 400 - 550 and 550 - 667 $\mathrm{cm^{-1}}$) for REFIR-PAD extension itself, REFIR-PAD extension based on LBLRTM (LBL), based on LBLRTM + noise (LBN) and based on coupled LBLRTM (LBC). The first and second lines correspond to a linear and a logarithmic extension respectively. The values correspond to the median value $\pm$ 1 σ.

	[100.4;400]		[400;550]		[550;667]	
	[%]	[r.u.]	[%]	[r.u.]	[%]	[r.u.]
REFIR-PAD	0.2 $\pm$ 3.9	0.1 $\pm$ 1.8	0.0 $\pm$ 13.0	0.0 $\pm$ 2.0	-2.2 $\pm$ 3.4	-0.8 $\pm$ 1.3
	-1.1 $\pm$ 5.9	-0.4 $\pm$ 2.3	3.0 $\pm$ 9.2	0.6 $\pm$ 1.8	0.2 $\pm$ 2.1	0.1 $\pm$ 0.9
LBL	-14.4 $\pm$ 17.4	-5.5 $\pm$ 7.6	-124.3 $\pm$ 143.5	-20.8 $\pm$ 19.1	-35.4 $\pm$ 33.3	-12.7 $\pm$ 10.5
	-13.4 $\pm$ 17.0	-5.5 $\pm$ 5.9	-105.5 $\pm$ 123.5	-18.0 $\pm$ 17.0	-37.5 $\pm$ 46.0	-12.9 $\pm$ 16.5
LBN	4.6 $\pm$ 4.5	2.2 $\pm$ 1.9	-0.1 $\pm$ 16.6	0.0 $\pm$ 2.6	-1.9 $\pm$ 3.6	-0.7 $\pm$ 1.3
	3.0 $\pm$ 5.0	1.2 $\pm$ 2.1	0.4 $\pm$ 15.8	0.1 $\pm$ 2.7	-3.4 $\pm$ 4.3	-1.3 $\pm$ 1.6
LBC	1.3 $\pm$ 5.7	0.5 $\pm$ 2.2	-6.3 $\pm$ 17.1	-1.3 $\pm$ 2.3	-4.4 $\pm$ 3.2	-1.7 $\pm$ 1.1
	1.4 $\pm$ 6.0	0.6 $\pm$ 2.5	-18.8 $\pm$ 29.7	-2.6 $\pm$ 5.1	-4.9 $\pm$ 3.3	-1.9 $\pm$ 1.1

seen, we choose to keep our vertical profiles. With this approach, biases between the observations and the corresponding simulations are within 2 r.u., consistent with Rizzi et al. (2018).

In this study, the extension of REFIR-PAD has been performed on its native grid ($\Delta\nu$ = 0.4 $\mathrm{cm^{-1}}$) and the results have been predominantly presented over averaged bands of $\Delta\nu$ = 10 $\mathrm{cm^{-1}}$. At present, climate and Earth-system models do not operate at such a high spectral resolution. It is thus of interest to investigate how the differences presented in figures 4 and 6 are affected by integration over the wider spectral bands more typical of these general circulation models. As an exemplar, we consider the Met Office Unified Model (UM). In the UM, there are three bands with FIR contributions, from 1 - 400, 400 - 550 and 550 - 800 $\mathrm{cm^{-1}}$.

The extensions of REFIR-PAD using the various prediction models described in section 3.2 were integrated over these bands and the corresponding results are shown in table 1. For each band and each case, the median value of the variations is provided along with the one sigma standard deviation of the relative variation across spectra in the test set. Because of the boundaries of the extension, the bands from 1 - 400 $\mathrm{cm^{-1}}$ and 550 - 800 $\mathrm{cm^{-1}}$ are reduced to 100.4 - 400 $\mathrm{cm^{-1}}$ and 550 - 667 $\mathrm{cm^{-1}}$ respectively.

Using the REFIR-PAD prediction model, integrating over wide spectral bands results in relatively small differences between the observed and extended spectra, below 3 %. However, as described earlier, the extension using simulated noise-free regression coefficients leads to strong biases, with maximum percentage differences (up to -119 %) seen in the 400-550 $\mathrm{cm^{-1}}$ region, the most transparent of the three bands and hence the most susceptible to noise due to the low radiance level. When looking at LBN and LBC cases, the extension shows median biases which are only marginally larger than those seen using the observations themselves. In addition, the difference between using a linear or logarithmic extension is small.

5 Conclusions

In this study we have used REFIR-PAD downwelling radiance observations covering the spectral range 100-1400 cm^{-1} for clear-sky cases from 2013 over Dome C in Antarctica to assess whether it is currently possible to build a model which uses MIR spectral radiances to predict spectral values in the FIR to an acceptable level of accuracy. The motivation for this work comes from a number of studies that have estimated the FIR spectrum from satellite observations of MIR radiances (Huang et al., 2008; Turner et al., 2015). While these have shown encouraging agreement with broadband observations the results have not been tested with spectrally resolved measurements due to the lack of such observations. We have described a correlation and regression based methodology based on Turner et al. (2015) which we have used to search for predictor wavenumbers and to extract regression coefficients at these specified wavenumbers. In addition to the observations, radio-sonde soundings are used to create a corresponding simulated spectral database with the radiative transfer model LBLRTM.

Correlation maps between the observed FIR and MIR radiances show peak values at wavenumbers around 700 cm^{-1}. In constrast, noise-free simulated spectra show peak correlations at wavenumbers between 1340 and 1400 cm^{-1}. With the addition of realistic noise to the simulations the pattern of the correlation map alters and looks more similar to the one created using the REFIR-PAD observations, with reduced correlations at wavenumbers < 180 cm^{-1}, between 470-570 cm^{-1} and between 1340-1400 cm^{-1}. This indicates that the selected wavenumbers and the associated MIR to FIR correlation are both highly dependent on instrumental noise. One possible way of at least partially mitigating these noise effects would be to combine channels showing the highest correlations such that the predictors for a given FIR channel comprise contributions from more than one MIR measurement. This could certainly be an area for future investigation.

Using a prediction model built solely with REFIR-PAD observations, the extension from the MIR to the FIR works satisfactorily, with mean relative variations below 5 % over most of the spectral range. Between 400 and 570 cm^{-1}, where the atmosphere is highly transparent and the downwelling radiances are very low, the relative variation can reach up to 10 % but the absolute variation is of the same order to the rest of the spectrum (0.5 r.u.). Using a prediction model based on noise-free simulations, the extension to the FIR shows markedly poorer fidelity with the observed behaviour. However, when we add realistic instrument noise to the simulations the prediction model is able to satisfactorily estimate the REFIR-PAD FIR measurements. Where the radiance is low, higher relative differences can arise as for the REFIR-PAD only case. Notable differences are also seen at wavenumbers below 150 cm^{-1} which can be explained by the enhanced instrument noise close to the edge of the REFIR-PAD detector.

Our results show that while it is feasible to use the type of approach we have outlined here to extend mid infrared spectral measurements to the far infrared, the quality of the extension is strongly dependent on the noise characteristics of the observations. This in turn implies that if a similar approach is developed to extend existing mid infrared ground or satellite based observations, the instrument noise must be explicitly accounted for in building the model due to its potential role in altering the choice of predictor wavenumbers from the noise-free case. In addition, the quality of any extension using this type of method will also be critically dependent on whether the creation set of atmospheric profiles correctly represents the conditions which are actually sampled by the MIR instruments.

An obvious next step for this work would be to include cloudy conditions in the approach. However, this is challenging, as, given the results here, one would anticipate that a good knowledge of cloud microphysics, optical properties as well as vertical location, including any impact on the associated temperature and water vapour profiles, would be required to perform the forward modelling with the requisite accuracy. The frequency of radiosonde ascents at Concordia preclude knowledge of the last effect. Cloud microphysics are not measured directly, cirrus bulk optical properties are poorly constrained in the FIR (Baran et al., 2014) and previous campaigns highlight the difficulty in matching radiance measurements across the infrared in the presence of cirrus cloud (Cox et al., 2010). However, retrievals directly from the REFIR-PAD measurements themselves may provide a means to circumvent some of these issues in future (Di Natale et al., 2017; Maestri et al., 2018).

More generally, one would want to test whether such a synthetic approach could be applied at the global scale and for potentially more interesting satellite viewing geometries. If selected, the candidate ESA Earth Explorer 9 mission, the Far infrared Outgoing Radiation Understanding and Monitoring concept (FORUM, Palchetti et al., 2016) could provide the extensive, simultaneous FIR and MIR observational database needed to build and validate such a prediction model at the spectrally resolved level. With a correct appreciation of the role of instrument noise, such a model could then be applied retrospectively to existing MIR hyperspectral measurements (such as IASI) to derive a long-term record of spectrally resolved radiances suitable for climate model evaluation.

Competing interests. The authors declare that they have no conflict of interest.

Acknowledgements. The analysis was supported by the NERC-funded International Consortium for the Exploitation of Infrared Measurements of PolAr ClimaTe (ICE-IMPACT) project (grant NE/N01376X/1) and by the National Centre for Earth Observation, UK. The deployment of REFIR-PAD in Antarctica was supported by the Italian National Program for Research in Antarctica PNRA (Programma Nazionale di Ricerche in Antartide) under the following projects: 2009/A04.03, 2013/AC3.01 and 2013/AC3.06. The REFIR-PAD data are available from http://refir.fi.ino.it/refir-pad-domeC. Radiosounding measurements are part of the IPEV/PNRA Project "Routine Meteorological Observation" at Station Concordia-www.climantartide.it/index.php?lang=enea. ECMWF data were acquired from http://www.ecmwf.int/en/research/climate-reanalysis/erainterim.

References

Anderson, G. P.: AFGL atmospheric constituent profiles (0-120km), 1986.

Baran, A. J., Hill, P., Furtado, K., Field, P., and Manners, J.: A Coupled Cloud Physics–Radiation Parameterization of the Bulk Optical Properties of Cirrus and Its Impact on the Met Office Unified Model Global Atmosphere 5.0 Configuration, Journal of Climate, 27, 7725–7752, https://doi.org/10.1175/JCLI-D-13-00700.1, https://doi.org/10.1175/JCLI-D-13-00700.1, 2014.

Bellisario, C., Brindley, H. E., Murray, J. E., Last, A., Pickering, J., Harlow, R. C., Fox, S., Fox, C., Newman, S. M., Smith, M., Anderson, D., Huang, X., and Chen, X.: Retrievals of the Far Infrared Surface Emissivity Over the Greenland Plateau Using the Tropospheric Airborne Fourier Transform Spectrometer (TAFTS), Journal of Geophysical Research: Atmospheres, 122, 12,152–12,166, https://doi.org/10.1002/2017JD027328, http://dx.doi.org/10.1002/2017JD027328, 2017JD027328, 2017.

Bianchini, G., Palchetti, L., and Carli, B.: A wide-band nadir-sounding spectroradiometer for the characterization of the Earth's outgoing long-wave radiation, https://doi.org/10.1117/12.689260, http://dx.doi.org/10.1117/12.689260, 2006.

Bianchini, G., Palchetti, L., Muscari, G., Fiorucci, I., Di Girolamo, P., and Di Iorio, T.: Water vapor sounding with the far infrared REFIR-PAD spectroradiometer from a high-altitude ground-based station during the ECOWAR campaign, Journal of Geophysical Research: Atmospheres, 116, n/a–n/a, https://doi.org/10.1029/2010JD014530, http://dx.doi.org/10.1029/2010JD014530, d02310, 2011.

Canas, T. A., Murray, J. E., and Harries, J. E.: Tropospheric airborne Fourier transform spectrometer (TAFTS), in: Satellite Remote Sensing of Clouds and the Atmosphere II, edited by Haigh, J. D., vol. 3220 of *Proceedings of the SPIE*, pp. 91–102, https://doi.org/10.1117/12.301139, 1997.

Clerbaux, C., Boynard, A., Clarisse, L., George, M., Hadji-Lazaro, J., Herbin, H., Hurtmans, D., Pommier, M., Razavi, A., Turquety, S., Wespes, C., and Coheur, P.-F.: Monitoring of atmospheric composition using the thermal infrared IASI/MetOp sounder, Atmospheric Chemistry and Physics, 9, 6041–6054, https://doi.org/10.5194/acp-9-6041-2009, https://www.atmos-chem-phys.net/9/6041/2009/, 2009.

Clough, S., Shephard, M., Mlawer, E., Delamere, J., Iacono, M., Cady-Pereira, K., Boukabara, S., and Brown, P.: Atmospheric radiative transfer modeling: a summary of the AER codes, Journal of Quantitative Spectroscopy and Radiative Transfer, 91, 233 – 244, https://doi.org/http://dx.doi.org/10.1016/j.jqsrt.2004.05.058, http://www.sciencedirect.com/science/article/pii/S0022407304002158, 2005.

Cox, C. V., Murray, J. E., Taylor, J. P., Green, P. D., Pickering, J. C., Harries, J. E., and Last, A. E.: Clear-sky far-infrared measurements observed with TAFTS during the EAQUATE campaign, September 2004, Quarterly Journal of the Royal Meteorological Society, 133, 273–283, https://doi.org/10.1002/qj.159, 2007.

Cox, C. V., Harries, J. E., Taylor, J. P., Green, P. D., Baran, A. J., Pickering, J. C., Last, A. E., and Murray, J.: Measurement and simulation of mid- and far-infrared spectra in the presence of cirrus, Quarterly Journal of the Royal Meteorological Society, 136, 718–739, https://doi.org/10.1002/qj.596, http://dx.doi.org/10.1002/qj.596, 2010.

Dee, D. P., Uppala, S. M., Simmons, A. J., Berrisford, P., Poli, P., Kobayashi, S., Andrae, U., Balmaseda, M. A., Balsamo, G., Bauer, P., Bechtold, P., Beljaars, A. C. M., van de Berg, L., Bidlot, J., Bormann, N., Delsol, C., Dragani, R., Fuentes, M., Geer, A. J., Haimberger, L., Healy, S. B., Hersbach, H., Hólm, E. V., Isaksen, L., Kållberg, P., Köhler, M., Matricardi, M., McNally, A. P., Monge-Sanz, B. M., Morcrette, J.-J., Park, B.-K., Peubey, C., de Rosnay, P., Tavolato, C., Thépaut, J.-N., and Vitart, F.: The ERA-Interim reanalysis: configuration and performance of the data assimilation system, Quarterly Journal of the Royal Meteorological Society, 137, 553–597, https://doi.org/10.1002/qj.828, http://dx.doi.org/10.1002/qj.828, 2011.

Di Natale, G., Palchetti, L., Bianchini, G., and Del Guasta, M.: Simultaneous retrieval of water vapour, temperature and cirrus clouds properties from measurements of far infrared spectral radiance over the Antarctic Plateau, Atmospheric Measurement Techniques, 10, 825–837, https://doi.org/10.5194/amt-10-825-2017, http://www.atmos-meas-tech.net/10/825/2017/, 2017.

Feldman, D. R., Collins, W. D., Pincus, R., Huang, X., and Chen, X.: Far-infrared surface emissivity and climate, Proceedings of the National Academy of Science, 111, 16 297–16 302, https://doi.org/10.1073/pnas.1413640111, 2014.

Fox, C., Green, P. D., Pickering, J. C., and Humpage, N.: Analysis of far-infrared spectral radiance observations of the water vapor continuum in the Arctic, Journal of Quantitative Spectroscopy and Radiative Transfer, 155, 57–65, https://doi.org/10.1016/j.jqsrt.2015.01.001, 2015.

Green, P. D., Newman, S. M., Beeby, R. J., Murray, J. E., Pickering, J. C., and Harries, J. E.: Recent advances in measurement of the water vapour continuum in the far-infrared spectral region, Philosophical Transactions of the Royal Society of London Series A, 370, 2637–2655, https://doi.org/10.1098/rsta.2011.0263, 2012.

Harries, J., Carli, B., Rizzi, R., Serio, C., Mlynczak, M., Palchetti, L., Maestri, T., Brindley, H., and Masiello, G.: The Far-infrared Earth, Reviews of Geophysics, 46, RG4004, https://doi.org/10.1029/2007RG000233, 2008.

Huang, X., Yang, W., Loeb, N. G., and Ramaswamy, V.: Spectrally resolved fluxes derived from collocated AIRS and CERES measurements and their application in model evaluation: Clear sky over the tropical oceans, Journal of Geophysical Research: Atmospheres, 113, n/a–n/a, https://doi.org/10.1029/2007JD009219, http://dx.doi.org/10.1029/2007JD009219, d09110, 2008.

Huang, X., Cole, J. N. S., He, F., Potter, G. L., Oreopoulos, L., Lee, D., Suarez, M., and Loeb, N. G.: Longwave Band-By-Band Cloud Radiative Effect and Its Application in GCM Evaluation, Journal of Climate, 26, 450–467, https://doi.org/10.1175/JCLI-D-12-00112.1, http://dx.doi.org/10.1175/JCLI-D-12-00112.1, 2013.

Maestri, T., Rizzi, R., Tosi, E., Veglio, P., Palchetti, L., Bianchini, G., Girolamo, P. D., Masiello, G., Serio, C., and Summa, D.: Analysis of cirrus cloud spectral signatures in the far infrared, Journal of Quantitative Spectroscopy and Radiative Transfer, 141, 49 – 64, https://doi.org/http://dx.doi.org/10.1016/j.jqsrt.2014.02.030, http://www.sciencedirect.com/science/article/pii/S0022407314000879, 2014.

Maestri, T., Arosio, C., Rizzi, R., Palchetti, L., and Bianchini, G.: Antarctic ice cloud identification and properties using downwelling spectral radiance from 100 to 1400 cm-1, submitted to Journal of Geophysical Research – Atmospheres, 2018JD029205, 2018.

Mast, J. C., Mlynczak, M. G., Cageao, R. P., Kratz, D. P., Latvakoski, H., Johnson, D. G., Turner, D. D., and Mlawer, E. J.: Measurements of downwelling far-infrared radiance during the RHUBC-II campaign at Cerro Toco, Chile and comparisons with line-by-line radiative transfer calculations, Journal of Quantitative Spectroscopy and Radiative Transfer, 198, 25 – 39, https://doi.org/https://doi.org/10.1016/j.jqsrt.2017.04.028, http://www.sciencedirect.com/science/article/pii/S0022407316308949, 2017.

Mlynczak, M. G., Johnson, D. G., Latvakoski, H., Jucks, K., Watson, M., Kratz, D. P., Bingham, G., Traub, W. A., Wellard, S. J., Hyde, C. R., and Liu, X.: First light from the Far-Infrared Spectroscopy of the Troposphere (FIRST) instrument, Geophysical Research Letters, 33, L07704, https://doi.org/10.1029/2005GL025114, 2006.

Mlynczak, M. G., Cageao, R. P., Mast, J. C., Kratz, D. P., Latvakoski, H., and Johnson, D. G.: Observations of downwelling far-infrared emission at Table Mountain California made by the FIRST instrument, Journal of Quantitative Spectroscopy and Radiative Transfer, 170, 90 – 105, https://doi.org/http://dx.doi.org/10.1016/j.jqsrt.2015.10.017, http://www.sciencedirect.com/science/article/pii/S0022407315300340, 2016.

Palchetti, L., Bianchini, G., Di Natale, G., and Del Guasta, M.: Far-Infrared Radiative Properties of Water Vapor and Clouds in Antarctica, Bulletin of the American Meteorological Society, 96, 1505–1518, https://doi.org/10.1175/BAMS-D-13-00286.1, 2015.

Palchetti, L., Di Natale, G., and Bianchini, G.: Remote sensing of cirrus cloud microphysical properties using spectral measurements over the full range of their thermal emission, Journal of Geophysical Research: Atmospheres, 121, 10,804–10,819, https://doi.org/10.1002/2016JD025162, http://dx.doi.org/10.1002/2016JD025162, 2016JD025162, 2016.

Rizzi, R., Arosio, C., Maestri, T., Palchetti, L., Bianchini, G., and Guasta, M. D.: One year of downwelling spectral radiance measurements from 100 to 1400 cm-1 at Dome Concordia: Results in clear conditions, Journal of Geophysical Research: Atmospheres, 121, 10,937–10,953, https://doi.org/10.1002/2016JD025341, https://agupubs.onlinelibrary.wiley.com/doi/abs/10.1002/2016JD025341, 2016.

Rizzi, R., Maestri, T., and Arosio, C.: Estimate of Radiosonde Dry Bias From Far-Infrared Measurements on the Antarctic Plateau, Journal of Geophysical Research: Atmospheres, 123, 3205–3211, https://doi.org/10.1002/2017JD027874, https://agupubs.onlinelibrary.wiley.com/doi/abs/10.1002/2017JD027874, 2018.

Rothman, L. S., Gordon, I. E., Babikov, Y., Barbe, A., Chris Benner, D., Bernath, P. F., Birk, M., Bizzocchi, L., Boudon, V., Brown, L. R., Campargue, A., Chance, K., Cohen, E. A., Coudert, L. H., Devi, V. M., Drouin, B. J., Fayt, A., Flaud, J.-M., Gamache, R. R., Harrison, J. J., Hartmann, J.-M., Hill, C., Hodges, J. T., Jacquemart, D., Jolly, A., Lamouroux, J., Le Roy, R. J., Li, G., Long, D. A., Lyulin, O. M., Mackie, C. J., Massie, S. T., Mikhailenko, S., Müller, H. S. P., Naumenko, O. V., Nikitin, A. V., Orphal, J., Perevalov, V., Perrin, A., Polovtseva, E. R., Richard, C., Smith, M. A. H., Starikova, E., Sung, K., Tashkun, S., Tennyson, J., Toon, G. C., Tyuterev, V. G., and Wagner, G.: The HITRAN2012 molecular spectroscopic database, Journal of Quantitative Spectroscopy and Radiative Transfer, 130, 4–50, https://doi.org/10.1016/j.jqsrt.2013.07.002, 2013.

Tomasi, C., Petkov, B., Benedetti, E., Valenziano, L., and Vitale, V.: Analysis of a 4 year radiosonde data set at Dome C for characterizing temperature and moisture conditions of the Antarctic atmosphere, Journal of Geophysical Research: Atmospheres, 116, n/a–n/a, https://doi.org/10.1029/2011JD015803, http://dx.doi.org/10.1029/2011JD015803, d15304, 2011.

Turner, D. and Mlawer, E.: The Radiative Heating in Underexplored Bands Campaigns, Bulletin of the American Meteorological Society, 91, 911–923, https://doi.org/10.1175/2010BAMS2904.1, http://dx.doi.org/10.1175/2010BAMS2904.1, 2010.

Turner, E. C., Lee, H.-T., and Tett, S. F. B.: Using IASI to simulate the total spectrum of outgoing long-wave radiances, Atmospheric Chemistry and Physics, 15, 6561–6575, https://doi.org/10.5194/acp-15-6561-2015, http://www.atmos-chem-phys.net/15/6561/2015/, 2015.

Wielicki, B. A., Barkstrom, B. R., Harrison, E. F., III, R. B. L., Smith, G. L., and Cooper, J. E.: Clouds and the Earth's Radiant Energy System (CERES): An Earth Observing System Experiment, Bulletin of the American Meteorological Society, 77, 853–868, https://doi.org/10.1175/1520-0477(1996)077<0853:CATERE>2.0.CO;2, https://doi.org/10.1175/1520-0477(1996)077<0853:CATERE>2.0.CO;2, 1996.

Yang, P., Mlynczak, M. G., Wei, H., Kratz, D. P., Baum, B. A., Hu, Y. X., Wiscombe, W. J., Heidinger, A., and Mishchenko, M. I.: Spectral signature of ice clouds in the far-infrared region: Single-scattering calculations and radiative sensitivity study, Journal of Geophysical Research: Atmospheres, 108, n/a–n/a, https://doi.org/10.1029/2002JD003291, http://dx.doi.org/10.1029/2002JD003291, 4569, 2003.